Dynamic polarization of nuclei in solid dielectrics

V. A. Atsarkin

Institute of Radio Engineering and Electronics, Academy of Sciences of the USSR, Moscow
Usp. Fiz. Nauk **126**, 3–39 (September 1978)

A review is given of the present state of the theory of dynamic nuclear polarization (DNP) by the dipole electron-nucleus interaction in solids. The two-particle (solid effect), three-particle (electron-nucleus cross relaxation), and many-particle (dynamic cooling) mechanisms of DNP are discussed both for idealized conditions and under inhomogeneous broadening of the ESR line. The effect of foreign impurities, spin diffusion, phonon bottlenecks, and very low temperatures is analyzed. The treatment is based on a unified approach based on the concepts of spin temperature and thermal mixing in a rotating coordinate frame. The review covers experimental data illustrating the DNP mechanisms, possible applications of this phenomenon in the development of highly polarized proton targets, and so on. A brief discussion is also given of other DNP methods and mechanisms (the Overhauser effect and optical nuclear polarization).

PACS numbers: 76.70.Ey, 77.30. + d

CONTENTS

INTRODUCTION

The phrase "dynamic nuclear polarization" (DNP) encompasses a range of phenomena and methods involving forced orientation of nuclear spins in a given direction under the influence of high-frequency fields.

The development of objects with a high degree of nuclear polarization is of considerable importance for elementary-particle physics, since such objects can be used to investigate the spin dependence of nuclear forces in scattering experiments. Moreover, DNP studies can substantially extend our understanding of the dynamics of spin systems and, in particular, provide valuable information on electron-nucleus interactions, spin-lattice relaxation, the energy spectrum, and other important characteristics of matter.

DNP methods which originated in the discovery of the Overhauser effect[1] have undergone rapid development during the last decade both in depth and scope. Thus, on the one hand, record levels of nuclear polarization have been achieved (nearly 100% for protons), so that it has been possible to develop highly effective polarized targets and neutron polarizers for use in nuclear physics.[2] It has also been possible to observe such unique physical phenomena as nuclear ferro- and antiferromagnetism.[3] On the other hand, detailed studies of the origin of DNP in solids have led to a clear understanding of the physics of this phenomenon in terms of the concept of spin temperature.[4] All these achievements have involved mainly solid dielectrics, where the DNP effect is based on the magnetic dipole interaction between the nuclei in the matrix and unpaired electrons in the paramagnetic impurity (this is the so-called solid effect and its varieties). Most published theoretical and experimental work on DNP has been devoted to these methods[2,4-7]: We shall also devote most of our attention to these topics.[1)]

One of our main aims is to provide a clear exposition of the various DNP mechanisms, to contrast and compare them, and to consider their common basis which we see in the model of thermal mixing in a rotating co-

[1)]This review covers papers published up to March 1977.

 0038-5670/78/090725-21$01.10

ordinate frame. In the interests of maximum possible simplicity, we have excluded questions connected with the quantum-statistics justification of the theory and have confined our attention to relatively simple and graphic physical considerations. Readers wishing to acquaint themselves with more rigorous treatment and, in particular, with the fundamentals of the idea of spin temperature are referred to the literature.[4,8-11]

1. DNP MECHANISMS INVOLVING THE ELECTRON-NUCLEAR DIPOLE INTERACTION

A. The system under investigation

The system under investigation in DNP experiments is a solid dielectric specimen containing n_I nuclei per unit volume, each having spin I, and n_S unpaired electrons, each with spin S. The specimen is placed in a constant magnetic field H_0 whose direction is parallel to the z axis. The unpaired electrons ("electron spins") may belong to paramagnetic impurity ions (for example, Cr^{3+}, Nd^{3+}, and so on), free radicals, optically excited triplet molecules, and so on. It will be assumed throughout that $N \equiv n_I/n_S \gg 1$.

To avoid unimportant complications, we assume that $S = I = 1/2$ and that the electron g factor is isotropic. The system under investigation is then characterized by the following spin Hamiltonian:

$$\hat{\mathcal{H}} = \hat{\mathcal{H}}_S + \hat{\mathcal{H}}_I + \hat{\mathcal{H}}_{SS} + \hat{\mathcal{H}}_{II} + \hat{\mathcal{H}}_{SI}, \qquad (1.1)$$

where $\hat{\mathcal{H}}_S = \hbar\omega_S \hat{S}^z$ and $\hat{\mathcal{H}}_I = -\hbar\omega_I \hat{I}^z$ are, respectively, the Zeeman energies of the spins S and I in the field H_0, where $\omega_S = -\gamma_S H_0$ and $\omega_I = \gamma_I H_0$ are the corresponding Larmor frequencies, and γ_S, γ_I are the gyromagnetic ratios (we assume that $\gamma_S < 0$, $\gamma_I > 0$); S^z and I^z are operators representing the resultant projections of spins S and I along the z axis, and $\hat{\mathcal{H}}_{SS}$, $\hat{\mathcal{H}}_{II}$, and $\hat{\mathcal{H}}_{SI}$ are the Hamiltonians representing the dipole-dipole interactions between the indicated spins.

The spin-lattice interaction, which is not included in the Hamiltonian given by (1.1), is usually taken into account with the aid of the phenomenological relaxation times τ_{SI} and τ_{II} for the spins S and I, respectively. It is assumed that the field H_0 is strong enough to enable us to characterize the energy levels of the system by wave functions $|m_S, M_I\rangle$, where m_S and m_I are the magnetic quantum numbers of the electrons and nuclei, respectively.

The polarization of the nuclei and electrons in the z direction is defined by

$$p = \frac{\langle I^z \rangle}{I} = \frac{n_I^+ - n_I^-}{n_I},$$

$$P = \frac{\langle S^z \rangle}{S} = \frac{n_S^+ - n_S^-}{n_S},$$

where $n_I^\pm$ and $n_S^\pm$ are the populations of the nuclear and electron energy levels with m_I, $m_S = \pm 1/2$. For equilibrium with the lattice at temperature T_0, we have

$$p^0 = \tanh\frac{\hbar\gamma_I H_0}{2kT_0} \approx \frac{\hbar\gamma_I H_0}{2kT_0}, \quad P^0 = \tanh\frac{\hbar\gamma_S H_0}{2kT_0} \approx \frac{\hbar\gamma_S H_0}{2kT_0}$$

(these approximations correspond to the "high-temperature" case p^0, $P^0 \ll 1$; this condition is realized in practise for $H_0/T_0 \lesssim 3\text{kOe}/^\circ\text{K}$, and will be assumed to be satisfied up to Sec. 3).

Hence, it is clear that, under equilibrium conditions, the electron polarization exceeds the nuclear polarization by the factor $|\gamma_S/\gamma_I|$, i.e., roughly three orders of magnitude. In the final analysis, all the DNP mechanisms reduce to the transfer of high electron polarization to the nuclear spins in the specimen and the difference between these mechanisms lies, in particular, in the number of particles participating in the elementary transfer event. Thus, in the solid effect (SE),[12] the result is achieved through electron-nuclear transitions, each of which involves only two spins, namely, S and I. In the case of DNP due to electron-nuclear cross relaxation (ENCR), three particles are involved in simultaneous spin flip (two electrons and one nucleus).[13] Finally, in the dynamic cooling (DC) mechanism,[10,14-16] nuclear polarization is due to the transfer of the collective energy of the electron spin-spin interactions to the nuclei, i.e., we have an essentially many-particle effect. We shall examine each of these three basic DNP mechanisms in its "pure" form in order to achieve maximum clarity in contrasting them.

B. Solid effect with allowed structure

The SE mechanism, first described by Abragam and Proctor[12] and Erb *et al.*,[17] has frequently been examined in review papers and monographs.[5,6,18] The DNP effect is achieved in this case by subjecting the specimen to a high-frequency field $2H_1 \cos\omega_p t$, which is linearly polarized at right-angles to H_0, and then exciting it with the aid of induced transitions at the frequencies $\omega_S + \omega_I$ or $\omega_S - \omega_I$, corresponding to the simultaneous spin flip by one electron and one nuclear spin in antiparallel or parallel directions. Such transitions are forbidden when $\hat{\mathcal{H}}_{SI}$ is absent from (1.1). The electron-nuclear interaction (in particular, the terms $\hat{S}^z\hat{I}^\pm$) partially remove this selection rule, so that the probability of such "forbidden" transitions for a given pair of spins S_i, I_j is

$$W_{ij}^\pm(\Delta_p) = \sigma_{ij} W(\Delta_p \mp \omega_I),$$

where $\Delta_p = \omega_p - \omega_S$, $W(x) = (\pi/2)(\gamma_S H_1)^2 g(x)$ is the probability of the usual "allowed" transitions with a change in only m_S, $g(x)$ is the form-factor for the ESR line, and σ_{ij} is the "forbiddenness factor" given by

$$\sigma_{ij} = \frac{9}{4}\frac{(\hbar\gamma_S)^2}{r_{ij}^6 H_0^2}\sin^2\theta_{ij}\cos^2\theta_{ij},$$

where r_{ij} is the radius vector connecting S_i and I_j and θ_{ij} is the angle between H_0 and r_{ij} (a common notation $\Gamma_{ij}^\pm \equiv W_{ij}^\pm r_{ij}^6$). Under typical conditions ($H_0 \sim 10^3$–10^4 Oe; $r_{ij} > 3$–5 Å), it is found that $\sigma_{ij} \ll 1$.

To ensure that the experimental conditions correspond to "pure" SE, one must induce only the "forbidden" transitions of a particular sign without exciting the purely electronic transitions. This is possible only when both types of transition are spectroscopically allowed, i.e., the width δ_S of the ESR line is much less than ω_I. We shall suppose, in this section, that this condition is satisfied and, moreover, $\omega_p = \omega_S \pm \omega_I$.

The energy-level scheme and the possible transitions in SE are shown in Fig. 1. It is clear that, when one of the "forbidden" transitions is saturated, the quantity p_j tends to $\pm P_i$, whereas, if the time τ_{Sl} is short enough to ensure that the electron spins remain in equilibrium with the lattice, then $p_j \to \pm P_i^0$, i.e., there is an increase in the nuclear polarization by the factor $|\gamma_S/\gamma_I|$.

To determine the DNP for the entire specimen, it is essential, in principle, to take into account the interaction of each of the spins S with all the spins I. However, this problem is simplified by two considerations.

Firstly, in solids maintained at low temperatures, nuclear spin-lattice relaxation is also produced through "forbidden" electron-nuclear transitions induced not by the high-frequency field but by the lattice vibrations.[5,6] Since, usually, $(\tau_{Sl}\omega_I)^2 \gg 1$, we have for the same pair S_i, I_j

$$(\tau_{Il})_{ij}^{-1} = \sigma_{ij}\tau_{Sl}^{-1} = C_{ij}r_{ij}^{-6}, \tag{1.2}$$

where C_{ij} are defined by analogy with Γ_{ij}. Thus, $W_{ij}^{\pm}$ and $(\tau_{Il})_{ij}^{-1}$ decrease rapidly with increasing r_{ij}, and we can therefore confine our attention to the interaction of each nucleus with its nearest electron and, instead of the entire specimen, we can consider one "sphere of influence" centered on the site i and having a mean radius $R = [(4/3)\pi n_S]^{-1/3}$.

Secondly, the interaction $\mathcal{H}_{II}$ (and, in particular, terms of the form $\hat{I}_i^+\hat{I}_j^-$) produces mutual spin flips among neighboring nuclei, which lead to the propagation of nuclear polarization in space by the diffusion law.[19-21] We assume, to begin with, that spin diffusion occurs rapidly enough to ensure that in a time interval less than $(\tau_{Il})_{ij}$ and $(W_{ij}^{\pm})^{-1}$ the values of p_j become equal throughout the sphere of influence, except for a small region of radius d centered on the spin S_i. This quantity d is called the radius of the diffusion barrier[20,21] and is determined from the condition that, for $r_{ij} < d$, the shift of the Larmor frequencies of neighboring nuclei due to the local static field of the spin S_i is greater than the width of the NMR line, so that such nuclei participate neither in spin diffusion nor in the "forbidden" induced transitions. The quantity σ_{ij}, $W_{ij}^{\pm}$, $\Gamma_{ij}^{\pm}$, $(\tau_{Il})_{ij}^{-1}$ and C_{ij} can then be replaced by σ, $W^{\pm}$, $\Gamma^{\pm}$, τ_{Il}^{-1} and C, averaged over the spherical shell with radii d and R:

$$\sigma = \frac{3}{10}\frac{(\hbar\gamma_S)^2}{H_0^2}(dR)^{-3}, \quad W^{\pm} = \sigma W \equiv \Gamma^{\pm}(dR)^{-3}, \quad \tau_{Il}^{-1} = \sigma\tau_{Sl}^{-1} = C(dR)^{-3}$$

Usually, $d \ll R$, so that most nuclei can be characterized by a single value of p. If we now use the principle

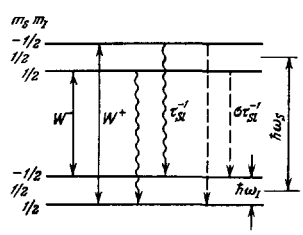

FIG. 1. Energy levels of electron and nucleus in the field H_0. Solid arrows—induced forbidden transitions, wavy arrows—electron spin-lattice relaxation, dashed arrows—forbidden relaxation transitions.

of detailed balancing, we can readily show that

$$\frac{dp}{dt} = -\frac{1}{\tau_{Il}}(p-p^0) - W^{\pm}(p \mp P),$$
$$\frac{dP}{dt} = -\frac{1}{\tau_{Sl}}(P-P^0) - NW^{\pm}(P \mp p). \tag{1.3}$$

Under stationary conditions, the nuclear polarization is given by

$$p_{st} = p^0\frac{1+fs^{\pm}}{1+s^{\pm}(1+f)} \pm p^0\frac{s^{\pm}}{1+s^{\pm}(1+f)}, \tag{1.4}$$

where $s^{\pm} = \Gamma^{\pm}/C$ is the saturation factor for the "forbidden" transition and $f = N\tau_{Sl}/\tau_{Il} = N\sigma$ is the so-called leakage factor (it can be shown that $f \ll 1$ in the absence of extraneous nuclear relaxation[22]). In the case of strong saturation ($s^{\pm} \gg 1$)

$$p_{st}^{\infty} = \pm p_{st}^{\infty} = \pm\frac{p^0}{1+f}, \tag{1.5}$$

i.e., the enhancement of nuclear polarization as compared with the equilibrium polarization, $E = p/p^0$, is

$$E^{\infty} = \pm\frac{\gamma_S}{\gamma_I(1+f)}, \tag{1.6}$$

and reaches its limiting value $E_{max} = \pm\gamma_S/\gamma_I$ for $f \ll 1$.

It is clear from (1.3) that the process of attainment of the stationary state is described by a function consisting of two exponentials, but, under the initial conditions $p(0) = p^0$, $P(0) = P^0$, the function $p(t)$ is practically a single exponential with time constant

$$\tau_p^{-1} = \tau_{Il}^{-1}\left(1+\frac{s^{\pm}}{1+fs^{\pm}}\right).$$

For $s^{\pm} \to \infty$, we then have

$$\tau_p^{\infty} = \tau_{Il}\frac{f}{1+f}, \tag{1.7}$$

but, when $f \ll 1$, it is, in practice, difficult to take $s^{\pm}$ to values of the order of $1/f$, so that one is interested in the case where $s^{\pm} \ll 1/f$ for which

$$\tau_p \approx \frac{\tau_{Il}}{1+s^{\pm}} = \frac{R^3d^3}{C(1+s^{\pm})}. \tag{1.8}$$

C. The role of spin diffusion and foreign impurities

When nuclear spin diffusion is not as effective as was assumed above, it must be taken explicitly into account. This problem has been investigated in detail in the literature 20, 21, 23–27 and we shall therefore confine our attention to summarizing the leading results.

When $r_{ij} \gg a$ (a is the minimum separation between nuclei), we can replace the true spatial distribution of nuclear polarization $p(r_{ij})$ by a continuous distribution $p(r)$ for which, under the conditions prevailing in SE, we have the diffusion equation (we confine our attention to a single sphere of influence)

$$\frac{\partial p(r,t)}{\partial t} = D\nabla^2 p(r,t) - \frac{C}{r^6}[p(r,t)-p^0] - \frac{\Gamma^{\pm}}{r^6}[p(r,t) \mp P(t)], \tag{1.9}$$

where $D \sim 0.1a^2\tau_{2I}^{-1}$ is the spin diffusion coefficient and τ_{2I} is the time of transverse relaxation of spins I. In principle, this differential equation must be solved simultaneously with the corresponding equation for $P(t)$, but one usually neglects the influence of nuclear polari-

zation on electron polarization, assuming that the attainment of P_{st} proceeds much more rapidly than the attainment of P_{st} (this is the case for fast diffusion if $s^{\pm} \ll 1/f$). In this approximation, we can replace $P(t)$ in (1.9) by $P_{st} = P_0$, and take the nuclear polarization $\bar{p}$ averaged over the volume, for which we have the simple equation

$$\frac{d\bar{p}}{dt} = -\frac{1}{\tau_p}(\bar{p} - p_{st}).$$

The quantity p_{st} is now defined by the same formula as in the case of fast diffusion, namely, (1.4). This was to be expected because, in the absence of extraneous nuclear relaxation, the ratio $W^{\pm}_{ij}/(\tau_{Il})^{-1}_{ij}$ is independent of r^{-1}_{ij}, so that all the p_j are equal in the stationary state, and spin diffusion is unimportant. On the other hand, the time τ_p depends on the ratio of d to the "pseudopotential radius" [20]

$$b = 0.68\left(\frac{C+\Gamma^{\pm}}{D}\right)^{1/4}.$$

When $a,\ b \ll d \ll R$, we have the results given by (1.8). If, on the other hand, $a,\ d \ll b \ll R$ ("restricted diffusion"), then τ_p differs from the expression given by (1.8) only by the replacement of d^3 by $1.6b^3$, which yields the characteristic dependence of τ_p on the pump: $\tau_p \propto (1+s^{\pm})^{1/4}$. Finally, when $b \leq R$, transient processes become essentially nonexponential.[28]

We now anticipate our discussion below and note that, for other DNP mechanisms (ENCR and DC), spin diffusion is taken into account in a similar fashion, and we shall therefore not consider this henceforth any further. We note, however, that, in these cases, the assumption that the evolution of $p(t)$ and $P(t)$ is independent is less well founded, and this problem still awaits its final solution.

We now reproduce approximate formulas for d:[20, 24-26]

$$d = \begin{cases} (\gamma_S/\gamma_I)^{1/4} a & \text{for } \tau^{\varepsilon}_S > \tau_{sI}, \\ (P\gamma_S/\gamma_I)^{1/4} a & \text{for } \tau^{\varepsilon}_S < \tau_{sI}, \end{cases} \tag{1.10}$$

where τ^{ε}_S is the total correlation time for S^{ε} and is given by

$$(\tau^{\varepsilon}_S)^{-1} = \tau_{Si}^{-1} + \tau_S^{-1},$$

and τ_S is the correlation time for S^{ε} due to electron spin-spin interactions. It is clear from (1.10) that a reduction in P (for example, in the case of saturation of allowed transitions) leads to the "breakup" of the diffusion barrier.[26] This is particularly important for ENCR and DC mechanisms. Moreover, the quantity d is actually anisotropic and, for certain angles Θ_{ij}, falls very substantially. Finally, spin diffusion turns out to be possible (although retarded) even for $r_{ij} < d$, and the energy difference between a pair of nuclear spins undergoing spin slip can be compensated either at the expense of the lattice[29,30] or the energy $\hat{H}_{SS}$.[31] All this seriously weakens the importance of the diffusion barrier for DNP.

So far, we have assumed that the spins S are the only source of nuclear spin-lattice relaxation. If there are other relaxation mechanisms as well, and if they are spatially inhomogeneous (quadrupole relaxation, motion of nuclei, and so on), the corresponding velocity is simply added to τ^{-1}_{Il}, which produces an increase in f and a reduction in p_{st},[20] although, at low temperatures, these relaxation mechanisms are usually unimportant. If, on the other hand, the specimen contains n'_S undesirable electron spins S' (i.e., those not used for DNP) with relaxation time τ'_{Sl}, these spins must be given their own spheres of influence within which $(\Gamma^{\pm})' = 0$ and $\tau'_{Il} = \tau'_{Sl}/\sigma$.

A general analysis of this situation is complicated and we shall therefore consider two limiting cases, namely, the model of isolated spheres of influence and the model of uniform polarization.

In the former model, it is assumed that, in the "useful" spheres, p_{st} is determined from (1.4) and (1.5) whereas, in the "undesirable" spheres, $p'_{st} = p_0$. If we suppose that the volumes of all these spheres are the same (Fig. 2a), the mean specimen polarization $\bar{p}$ is given by

$$\bar{p}_{st} = \frac{n_S p_{st} + n'_S p^0}{n_S + n'_S}, \tag{1.11}$$

and hence

$$\bar{E}^{\infty} = \pm \frac{\gamma_S}{\gamma_I} \frac{n_S}{n_S + n'_S}.$$

A more rigorous approach is, however, to assume that the volume of each sphere of influence is determined by the number of nuclei which can "serve" a given electron spin, i.e., it is proportional to τ_p^{-1} for spins S and $(\tau'_{Il})^{-1}$ for spins S' (Fig. 2b). Instead of (1.11), we then have

$$\bar{p}_{st} = \frac{n_S \tau_p^{-1} p_{st} + n'_S (\tau'_{Il})^{-1} p^0}{n_S \tau_p^{-1} + n'_S (\tau'_{Il})^{-1}} = \frac{b n_S p_{st} + b' n'_S p^0}{n_S b + n'_S b'}, \tag{1.12}$$

where the second equation is valid for limited spin diffusion within each of the spheres of influence.

Generalization of (1.12) to several spins S', S'', ... is obvious.

In the other limiting case, i.e., the case of uniform polarization, spin diffusion is assumed to be sufficiently fast to ensure that p can be regarded as uniform throughout the volume at each instant of time (with the exception of small spheres of radius d; see Fig. 2c). It is readily shown that the value of p_{st} in this case is determined by a formula analogous to (1.4), but with the addition of the term $n'_S \tau_{sI}/n_S \tau'_{sI}$ to the denominator, so that a much larger pump is necessary to achieve the same polarization.

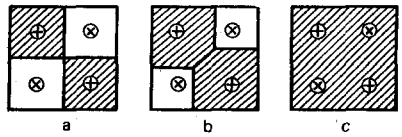

FIG. 2. Spheres of influence of "useful" (upright crosses) and "harmful" (oblique crosses) electron spins: a—equal-volume isolated spheres of influence, b—same model with larger spheres of "useful" spins, c—uniform polarization model. Regions of enhanced nuclear polarization are shaded.

D. Another approach: thermal mixing in a rotating coordinate frame

We now return to the model of fast diffusion in the absence of extraneous spins S, i.e., to equations (1.3). The spin system is now in quasiequilibrium at all times, and this enables us to introduce for each Zeeman subsystem Z_I and Z_S the corresponding terms $\mathcal{H}_I$ and $\mathcal{H}_S$ in (1.1) and the spin temperatures $T_I \equiv \beta^{-1}$ and $T_S \equiv \beta_S^{-1}$, given by

$$p = \tanh\frac{\hbar\omega_I}{2kT_I} \approx \frac{\hbar\gamma_I H_0}{2kT_I}, \quad P = -\tanh\frac{\hbar\omega_S}{2kT_S} \approx \frac{\hbar\gamma_S H_0}{2kT_S}. \tag{1.13}$$

In the language of quantum statistics, this corresponds to the density matrix

$$\hat{\rho} = \text{const}\cdot\exp\left(-\frac{\beta_I\hat{\mathcal{H}}_I}{k} - \frac{\beta_S\hat{\mathcal{H}}_S}{k}\right)$$
$$\approx \text{const}\cdot\left(1 - \frac{\beta_I\hat{\mathcal{H}}_I}{k} - \frac{\beta_S\hat{\mathcal{H}}_S}{k}\right)\ldots \tag{1.14}$$

(the energy of spin-spin interactions is not, so far, explicitly taken into account, and their contribution is restricted to participation in the establishment of quasiequilibrium).

We now transform to a coordinate frame rotating about the z axis with frequency ω_p in the direction of the Larmor precession of spins S, which corresponds to the canonical transformation performed with the aid of the unitary operator[5] $\hat{U} = \exp(i\omega_p\hat{S}^z t$. It is well known that the field H_0 acting on the spins S in this rotating coordinate frame is reduced to Δ_p/γ_S which, according to (1.13), is equivalent to the reduction of T_S to T_S^* $= -T_S\Delta_p/\omega_S$ (we assume that $|\gamma_S H_1| \ll \Delta_p$, δ_S), so that T_I remains unaltered.

We now introduce the notation

$$c_I = -\frac{d}{d\beta_I}\langle\hat{\mathcal{H}}_I\rangle, \quad c_S^* = -\frac{d}{d\beta_S^*}\langle\hat{\mathcal{H}}_S^*\rangle,$$

where the angle brackets represent mean values and the asterisk indicates that the corresponding quantities are taken in the rotating coordinate frame. It is readily verified that

$$c_I = \frac{\hbar^2 n_I I(I+1)\omega_I^2}{3k}, \quad c_S^* = \frac{\hbar^2 n_S S(S+1)\Delta_p^2}{3k},$$

where $c_I \gg c_S^*$.

We now rewrite (1.3) by expressing all the quantities in terms of β_I, β_S^*, c_I, and c_S^*, and taking into account the fact that $I = S = 1/2$ and $\Delta_p = \pm\omega_I$:

$$\frac{d\beta_I}{dt} = -\frac{1}{\tau_{Il}}(\beta_I - \beta_I^0) - W^{\pm}(\beta_I - \beta_S^*),$$
$$\frac{d\beta_S^*}{dt} = -\frac{1}{\tau_{Sl}}[\beta_S^* - (\beta_S^*)^0] - \frac{c_I}{c_S^*}W^{\pm}(\beta_S^* - \beta_I), \tag{1.15}$$

where $\beta_I^0 = \beta^0 = 1/T_0$ and $(\beta_S^*)^0 = -\beta^0\omega_S/\Delta_p$ is the reciprocal temperature of the lattice in the rotating coordinate frame.

The system of equations given by (1.15) is formally identical with the equations describing the usual heat transfer between two bodies (heat sources) with specific heats c_S^*, c_I, and temperatures β_S^*, β_I, in thermal contact with one another and with two thermostats, namely, the "source" and the "sink" at temperatures $(\beta_S^*)^0$ and β_I^0, respectively (Fig. 3). The fact that, instead of the usual temperatures, we now have the reciprocal spin

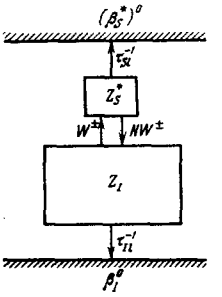

FIG. 3. Thermal mixing scheme for the solid effect.

temperatures clearly has no effect on the character of the process described by (1.15), which can be described as "thermal mixing".

The heat-balance equation now follows from (1.15):

$$\frac{d}{dt}\left(c_I\beta_I + c_S^*\beta_S^*\right) = -c_I\tau_{Il}^{-1}(\beta_I - \beta^0) - c_S^*\tau_{Sl}^{-1}[\beta_S^* - (\beta_S^*)^0]. \tag{1.16}$$

In isolation from the lattice, the right-hand side of this equation is, of course, zero, and the equation itself represents conservation of energy for thermal contact between Z_I and Z_S^*.

If the thermal contact between these subsystems is stronger than their coupling to the lattice, i.e., $\tau_{Il}W^{\pm} \gg 1$, then β_I and β_S^* rapidly assume the common value β^*. Substituting this into (1.16), we obtain

$$\frac{d}{dt}\beta^* = -\frac{1}{\tau_p}(\beta^* - \beta_{st}^*), \tag{1.17}$$

where

$$\beta_{st}^* = \frac{c_I\tau_{Il}^{-1} + c_S^*\tau_{Sl}^{-1}(\beta_S^*)^0}{c_I\tau_{Il}^{-1} + c_S^*\tau_{Sl}^{-1}}, \tag{1.18}$$

and the rate of the process is given by

$$\tau_p^{-1} = \frac{c_I\tau_{Il}^{-1} + c_S^*\tau_{Sl}^{-1}}{c_I + c_S^*}. \tag{1.19}$$

The expressions given by (1.18) and (1.19) are, of course, identical with the well-known expressions given by (1.5) and (1.7) for p_{st}^{∞} and τ_p^{∞}. Nevertheless, the above approach to SE is valuable because it enables us to view the situation from a different standpoint. Thermal mixing between Z_I and Z_S has a clear physical interpretation: the two subsystems have very close proper frequencies in the rotating coordinate frame (they are equal for $\Delta_p = \pm\omega_I$), so that, if there is contact produced by the saturation of "forbidden" transitions, resonance energy transfer will occur between them.

Although this approach appears to be relatively artificial, it is, in fact, very useful in the analysis of more complicated DNP mechanisms because it enables us to determine p_{st}^{∞} and τ_p directly from (1.18) and (1.19), providing only that one knows the "heat capacities" of the corresponding subsystems, and there are physical mechanisms capable of ensuring energy transfer between them.

In conclusion, we list the main distinguishing features of DNP in the case of the solid effect:

1. The reason for the polarization of nuclei in SE is the high-frequency saturation of "forbidden" transitions at frequencies $\omega_S \pm \omega_I$.

2. The result of SE is the establishment of the equal-

ity $p = \pm P$.

3. The maximum nuclear polarization in SE is $\pm P^0$ and, consequently, is independent of γ_I.

4. SE may be looked upon as thermal mixing between subsystems Z_I and Z_S^*.

E. Electron-nuclear cross relaxation (ENCR)

The nuclear polarization mechanism in the case of ENCR was proposed by Kessenikh and Manenkov[13] and was subsequently frequently discussed in connection with the interpretation of experiments.[32-34] This DNP mechanism arises if there are at least two types of electron spin, S_1 and S_2, the Larmor frequencies of which, ω_1 and ω_2, satisfy the relation

$$\Delta_{12} \equiv \omega_1 - \omega_2 \approx \pm\omega_I.$$

ENCR occurs as a result of the simultaneous operation of $\hat{\mathcal{H}}_{SS}$ and $\hat{\mathcal{H}}_{SI}$. The elementary event in this process is the simultaneous spin flip of all three particles: the spin S_1, the spin S_2, and the nuclear spin I at constant total Zeeman energy. The tendency for ENCR is to reach the equality

$$p = \pm(P_1 - P_2),$$

where P_1, P_2 are the polarizations of the spins S_1, S_2. If one of the ESR lines is saturated under these conditions by the high-frequency field of frequency, say, $\omega_p = \omega_1$, then $P_1 \to 0$ and $p \to \pm P_2$, which is very similar to the result in SE. We emphasize, however, that, in this case, it is sufficient to excite allowed (and not the forbidden) transitions. The ENCR picture is usually complicated by the simultaneous operation of the pure electron two-spin cross relaxation between S_1 and S_2.[35] Which of the two types of cross-relaxation is successful in this competition depends on the relationship between their probabilities $w^*(\Delta_{12})$ and $w_{CR}(\Delta_{12})$, where the ENCR probability is $w^*(\Delta_{12}) \sim \sigma w_{CR}(\Delta_{12} \mp \omega_I)$,[36] and σ is the "forbiddenness factor" introduced above.

For "ideal" ENCR, i.e., for $\Delta_{12} = \omega_I$ and when electron cross-relaxation and saturation of "forbidden" transitions can be neglected, the equations for fast diffusion can readily be obtained (see sub-sec. B of Sec. 1):

$$\left.\begin{aligned}
\frac{d}{dt}P_1 &= -\tau_{S1}^{-1}(P_1 - P_1^0) - \frac{n_I}{n_{S_1}} w^+(P_1 - P_2 + p) - 2WP_1 \\
\frac{d}{dt}P_2 &= -\tau_{S1}^{-1}(P_2 - P_2^0) - \frac{n_I}{n_{S_2}} w^+(-P_1 + P_2 - p) \\
\frac{d}{dt}p &= -\tau_I^{-1}(p - p^0) - w^*(P_1 - P_2 + p),
\end{aligned}\right\} \quad (1.20)$$

where n_{S_1}, n_{S_2} are the numbers of spins S_1 and S_2 (to be specific, we assume that $\Delta_{12} > 0$, the rates of spin lattice relaxation of S_1 and S_2 are the same, and $S_1 = S_2 = 1/2$).

The equations given by (1.20) can be readily solved in the usual way,[37] yielding p_{st} and τ_p. However, we shall proceed in a different way, again adopting the idea of thermal mixing. Thus, we write the electron Zeeman part of the spin Hamiltonian

$$\hat{\mathcal{H}}_S = \hbar\omega_1 \hat{S}_1^z + \hbar\omega_2 \hat{S}_2^z$$

in the form

$$\hat{\mathcal{H}}_S = \hat{\mathcal{H}}_\Sigma + \hat{\mathcal{H}}_\Delta = \hbar\omega_0(\hat{S}_1^z + \hat{S}_2^z) + \hbar\Delta_{12}\left(\frac{n_{S_2}}{n_S}\hat{S}_1^z - \frac{n_{S_1}}{n_S}\hat{S}_2^z\right), \quad (1.21)$$

where $n_S = n_{S_1} + n_{S_2}$ and $\omega_0 = (n_{S_1}\omega_1 + n_{S_2}\omega_2)/n_S$ is the frequency of the "center of gravity" of the ESR spectrum.

The Hamiltonian given by (1.21) corresponds to the splitting of the electron spin system into the "resultant" (Σ) and the "difference" (Δ) energy reservoirs whose reciprocal temperatures are $\beta_\Sigma = (n_{S_1}\beta_{S_1}\omega_1 + n_{S_2}\beta_{S_2}\omega_2)/n_S\omega_0$ and $\beta_\Delta = (\beta_{S_1}\omega_1 - \beta_{S_2}\omega_2)/n_S\Delta_{12}$ and can be found[4] from (1.21) and (1.14). In the absence of the high-frequency field, the subsystem Σ does not participate in ENCR because the total Z component of spins S_1 and S_2 is conserved in this process. The subsystem Δ, on the other hand, does participate in ENCR, where its interaction with Z_I for $\Delta_{12} = \omega_I$ has a resonance character and leads to thermal mixing. Transforming to the rotating coordinate frame, as in sub-section D, we obtain the mixing scheme for the three subsystems, namely, Δ, Z_I, and Σ^*, in which the $\Sigma^* \leftrightarrow \Delta$ contact is ensured by the presence of the ESR-saturating high-frequency field (Fig. 4). As in SE, interaction with the lattice provides the cold "source" for the electron spins and the hot "sink" for the nuclear spins with reciprocal temperatures, respectively $(\beta_\Sigma^*)^0 = \beta^0\omega_0/\Delta_{p0}$ and β^0 (where $\Delta_{p0} = \omega_p - \omega_0$).

If the contacts between Δ, Z_I and Σ^* are more efficient than the coupling with the lattice, the entire spin system assumes a uniform temperature β^*, whose stationary value can be determined directly from the thermal balance condition by analogy with (1.16)–(1.18):

$$\beta_{st}^* = \frac{2k}{\hbar\omega_I} p_{st}^\infty = \frac{c_\Sigma^*\tau_{S1}^{-1}(\beta_\Sigma^*)^0 + c_\Delta\tau_{S1}^{-1}\beta^0 + c_I\tau_I^{-1}\beta^0}{c_\Sigma^*\tau_{S1}^{-1} + c_\Delta\tau_{S1}^{-1} + c_I\tau_I^{-1}} \approx -\beta^0\frac{\omega_0\Delta_{p0}}{\Delta_{p0}^2 + M_2 + f\omega_1^2}, \quad (1.22)$$

where $M_2 = n_{S_1}n_{S_2}\Delta_{12}^2/n_S^2$ is the second moment of the ESR spectrum with respect to ω_0, and $c_\Sigma^* = \hbar^2 n_S\Delta_{p0}^2/4k$ and $c_\Delta = \hbar^2 M_2 n_S/4k$.

It follows from (1.22) that, when $n_{S_1} = n_{S_2}$, we have $E^\infty = \gamma_S/\gamma_I(1 + 2f)$, which is almost identical with the SE result given by (1.6) (the appearance of the factor 2 in front of f is due to the fact that only half of the electrons spins are subject to saturation). The time τ_p can be obtained in the same way.

The main features of DNP in the case of ENCR are thus as follows:

1. The reason for the polarization of the nuclei is the simultaneous action of three-spin electron-nuclear cross relaxation and the saturation of allowed transitions on one of the ESR frequencies.

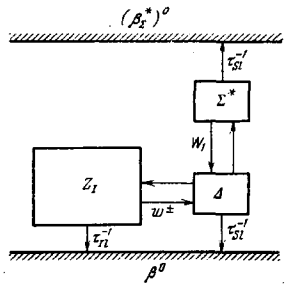

FIG. 4. Thermal mixing scheme for electron-nuclear cross-relaxation.

2. The result of ENCR is the establishment of the equation $p = \pm(P_1 - P_2)$.

3. The maximum achievable nuclear polarization is, as in SE, equal to $\pm P^0$.

4. DNP in the case of ENCR may be looked upon as thermal mixing between the subsystems Σ^*, Δ, and Z_I.

F. Dynamic cooling (DC)

This DNP mechanism is the most complex one because it necessitates the inclusion of the collective interaction between the electron spins in the specimen. Nuclear polarization now increases as a result of energy transfer between Z_I and the reservoir of electron spin-spin interactions which, in turn, is "cooled" during the saturation of ESR by the high-frequency field. The different DC mechanisms have been examined quantitatively by Kozhushner and Provotorov,[38] Buishvili,[15] Abragam and Borghini,[16] and others[4,39-41]

Let us suppose that the ESR line width δ_S is determined by electron spin-spin interactions. The absorption of a high-frequency quantum $\hbar\omega_p \equiv \hbar(\omega_S + \Delta_p)$ by the spin system can then be looked upon as the simultaneous transfer of energy $\hbar\omega_S$ to the reservoir Z_S and the remainder $\hbar\Delta_p$ to the so-called dipole-dipole reservoir (DDR) formed by the secular part $\hat{\mathcal{H}}^0_{SS}$ of the Hamiltonian $\hat{\mathcal{H}}_{SS}$ at the temperature[4,8] β_d^{-1} (see Fig. 5a).[2)]

This situation is very reminiscent of the simultaneous change in the energies of the subsystems Z_S and Z_I in the solid effect although we are now concerned not with the "forbidden" but with the allowed transitions and, instead of the subsystem Z_I with a unique resonance frequency ω_I, we have DDR which has a quasicontinuous spectrum in a range of the order of δ_S. It is therefore not surprising that the equations for β_S and β_d (first obtained by Provotorov[8a]) are very similar to the equations for SE given by (1.15):

$$\frac{d\beta_d}{dt} = -\tau_{dl}^{-1}(\beta_d - \beta^0) - 2W(\Delta_p)\frac{c_S^*}{c_d}(\beta_d - \beta_S^*), \tag{1.23a}$$

$$\frac{d\beta_S}{dt} = -\tau_{Sl}^{-1}[\beta_S - (\beta_S^*)^0] - 2W(\Delta_p)(\beta_S^* - \beta_d), \tag{1.23b}$$

where $c_d = -\langle\mathcal{H}^0_{SS}\rangle/\beta_d = \hbar^2 S(S+1)n_S\omega_d^2/3k$ and τ_{dl} and ω_d are, respectively, the spin lattice relaxation time and the mean DDR frequency (in the absence of extraneous paramagnetic impurities,[42] $\tau_{dl}/\tau_{Sl} \approx \omega_d^2/M_2^d$, where M_2^d is the second moment of the ESR line which, for pure dipole interaction,[5] is equal to $3\omega_d^2$).

It is obvious that (1.23) describes thermal mixing between Z_S^* and DDR in the rotating coordinate frame, which leads to the cooling of the latter. To obtain the DNP effect, it is sufficient to include the nuclear spins, i.e., the subsystem Z_I in this "refrigerating system."

We now have two different possibilities.

Firstly, the terms $\hat{S}_i^+\hat{S}_j^-$ in $\hat{\mathcal{H}}_{SS}$ ensure that the electron spins experience mutual spin flips with frequency

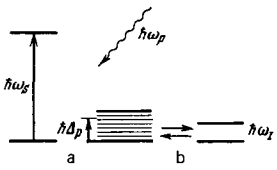

FIG. 5. Illustration of dynamic cooling mechanism. The quasi-continuous band is the DDR spectrum.

of the order of δ_S. Variable local fields, that arise as a result of this, act on the nuclear spins and, as in the case of spin lattice relaxation (see sub-sec. B, Section 1), give rise to nuclear transitions with mean (over the i-th sphere of influence) probability

$$w_{Id}^i = \frac{3}{40}\frac{(\hbar\gamma_S\gamma_I)^2}{d^3R^3}J_S^i(\omega_I) \equiv C_i^i(dR)^{-3}, \tag{1.24}$$

where $J_S^i(\omega_I)$ is the spectral density of the Fourier transform of the correlation function of the operator S_i^z at frequency ω_I [in the case of limited spin diffusion, d^3 must be replaced by $1.6b_{1i}^3$, where $b_{1i} = 0.68(C_1^i/D)^{1/4}$]. It is frequently assumed that the correlation is exponential with a common time[43] $\tau_S \sim 1/\delta_S$ for all i.[3)] We then have $J_S^i(\omega_1) = 2\tau_S/(1+\tau_S^2\omega_I^2)$ and, when $\tau_S\omega_I \gg 1$, we have $\tau_{Id}^{-1} \equiv 2w_{Id} = \sigma\tau_S^{-1}$, in complete analogy with (1.2).

Nuclear spin flip is accompanied in this process by the transfer of its Zeeman energy $\pm\hbar\omega_I$ to the DDR. The result of this energy transfer, which is most efficient for $\omega_I \sim \delta_S$, is clearly the establishment of a common temperature in DDR and Z_I (thermal mixing), leading to the DNP effect (Fig. 5b).

The above mechanism, which is called "direct contact" between Z_I and DDR, can also be interpreted in a different way. In point of fact, the change in the DDR energy by $\hbar\omega_I$ occurs in the simplest case as a result of the simultaneous spin flip in opposite directions of the two electron spins S_i and S_j, the energies of which in local fields differ by just $\hbar\omega_I$. Thus, if these local fields are static, the elementary "direct contact" event can be reduced to the three-spin ENCR considered in sub-section D.

When direct contact between Z_I and DDR is taken into account, the thermal mixing scheme in the rotating coordinate frame assumes the form illustrated in Fig. 6a and, when $W\tau_{Sl}$, $W\tau_{dl}$, $W_{Id}\tau_{Il} \gg 1$, we immediately have the result [compare this with (1.18) and (1.19)]

$$\beta_{st}^* = \frac{2k}{\hbar\omega_I}p_{st}^\infty = \frac{c_S^*\tau_{Sl}^{-1}(\beta_S^*)^0 + c_d\tau_{dl}^{-1}\beta^0 + c_I\tau_{Il}^{-1}\beta^0}{c_S^*\tau_{Sl}^{-1} + c_d\tau_{dl}^{-1} + c_I\tau_{Il}^{-1}} \approx -\frac{\beta^0\omega_S\Delta_p}{\Delta_p^2 + \omega_d^2\tau_{Sl}\tau_{dl}^{-1} + f\omega_I^2},$$
$$\tau_p^{-1} = \frac{c_s^*\tau_{sl}^{-1} + c_d\tau_{dl}^{-1} + c_I\tau_{Il}^{-1}}{c_s^* + c_d + c_I} \approx \tau_{Il}^{-1}\left(1 + \frac{\Delta_p^2 + \omega_d^2\tau_{sl}\tau_{dl}^{-1}}{f\omega_I^2}\right). \tag{1.25}$$

It is clear from (1.25) that the dependence of p_{st}^∞ on Δ_p has the characteristic "dispersion" form, i.e., the

[2)] We are using the traditional designation "dipole-dipole reservoir" (DDR) although $\hat{H}^0_{SS}$ may also include exchange interactions.

[3)] When the random distribution of the paramagnetic impurity is taken into account, each spin S_i has its own correlation time τ_s^i, and the correlation function averaged over all the electrons is proportional to $\exp(-A\sqrt{t})$, where A depends[44] on n_S and δ_S.

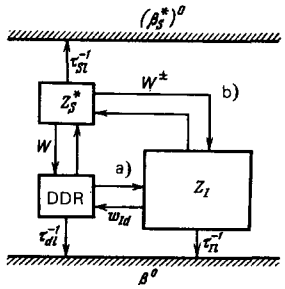

FIG. 6. Thermal mixing scheme for dynamic cooling: a—cooling by direct contact between Z_I and DDR, b—simultaneous saturation of allowed and "forbidden" transitions ("induced" contact).

DNP effect is absent for $\Delta_p = 0$ and has opposite signs on either side of this point. It is a maximum for $\Delta_p^{\max} \approx \omega_d \sqrt{\tau_{SI}/\tau_{dI}}$, where

$$|E_{\max}| = \frac{\omega_e}{2|\Delta_p^{\max}|} \gg 1. \tag{1.26}$$

It also follows from (1.25) that, when $f \ll 1$, the quantity $E_{\max}$ is practically independent of ω_I, in contrast to SE, for which $p_{\max}$ and not $E_{\max}$ is specified. Comparison of (1.26) with (1.6) shows that DC can, at least in principle, ensure a higher degree of polarization than SE, providing only[14] $2\omega_d \sqrt{\tau_{SI}/\tau_{dI}} < \omega_I$. However, because of the random distribution of the paramagnetic impurities, the ESR line shape in the case of the dipole broadening approaches the Lorentz form,[5] so that $\omega_d \gg \delta_S$ and the detuning $\Delta_p^{\max}$ corresponds to the distant wing of the line, where saturation is difficult to achieve.

The second method of transferring low temperature from DDR to the nuclei is the simultaneous saturation by the high-frequency field of: (a) an allowed electron transition for $\Delta_p \neq 0$ and (b) a "forbidden" transition[10] of a given sign.[4)] It is clear from the foregoing that process (a) leads to thermal mixing between Z_S^* and DDR, whereas (b) leads to mixing between the same subsystem Z_S^* and Z_I (see sub-section D and Fig. 6b). It is clear that, as a result of this "induced" contact, all three subsystems assume the same temperature, just as in the case of the direct contact which we have considered above.

An important feature of the "induced" contact between DDR and Z_I is that its efficiency is determined by the probability W^* and, consequently, is at the disposal of the experimenter, whereas, in the case of "direct" contact, it is proportional to w_{Id} and depends only on the properties of the specimen. We recall that, when $\delta_S < \omega_I$, so that it is difficult to achieve simultaneous saturation of both the allowed and forbidden transitions, an increase in p can be achieved with the aid of two high-frequency fields.[46]

In each of the above mechanisms of heat transfer between Z_I and DDR, it was assumed that cooling of the latter was ensured by the not strictly resonant saturation of the ESR line. This method, however, is not unique. An alternative approach involves the use of two electron spins S_1 and S_2 with frequencies ω_1 and ω_2, coupled by effective electron cross-relaxation. The elementary cross-relaxation event, which consists in the simultaneous spin flips of S_1 and S_2 in opposite directions, leads to the transfer of the energy $\hbar\Delta_{12}$ to DDR.[8b] By analogy with sub-section D, this may be looked upon as thermal mixing (with rate $\sim w_{CR}$) between DDR and the Δ-subsystem which, in turn, experiences mixing with the subsystem Σ^* during saturation of one of the ESR lines by the high-frequency field.

If we now add the nuclear spins and take into account the presence of either direct or induced contact between Z_I and DDR, we find that, in accordance with the scheme shown in Figs. 7a and b, and by analogy with (1.18), (1.22), and (1.25), the formula for the common temperature of the combined system $(\Sigma^* + \Delta + \mathrm{DDR} + Z_I)$ is

$$\beta_{st}^* \approx -\beta^0 \frac{\omega_0 \Delta_{p0}}{\Delta_{p0}^2 + M_2 + \omega_d^2 \tau_{sl} \tau_{dI}^{-1} + f\omega_I^2}. \tag{1.27}$$

We note that, when $\Delta_{12} \approx \omega_I$, there is one further possible mechanism for the equalization of β_d and β_I in this situation, namely, ENCR. In point of fact, it is shown in Sub-sec. E that this process mixes Z_I with the Δ subsystem which mixes with DDR through the pure electron cross-relaxation and the latter, in turn, mixes with the cooled subsystem Σ^* during the ESR saturation (Fig. 7c).

The untangling of this chain, which reminds one of "the house that Jack built," would require considerable effort, but this is precisely the power of the thermal mixing model: the result given by (1.27) is obtained directly and is independent of the sequence in which the various subsystems combine with one another.

Of course, as in any simplification, there are certain unavoidable defects: the mixing model will not allow us to determine p_{st} as a function of the high-frequency power or the probabilities w_{CR}, w_{Id}, and w^*. These functional relationships can only be obtained by solving the complete set of equations[10,14,15,40,41,45] for β_S^*, β_d, and β_I.

The entire foregoing discussion can be illustrated schematically as shown in Table I, which represents the various variants of the DC mechanism. Moreover, it is clear from this scheme that the overlap between the allowed and "forbidden" transitions ($\delta_S \gtrsim \omega_I$) leads to the transformation of SE into DC in the same way as ENCR

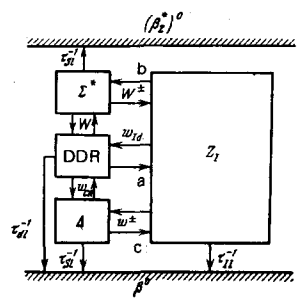

FIG. 7. Thermal mixing scheme for dynamic cooling in the case of electron cross-relaxation.

[4)] The necessary condition for this is $\omega_I \lesssim \delta_S$, which is opposite to the condition for the ideal SE (see sub-sec. B, Section 1).

TABLE I.

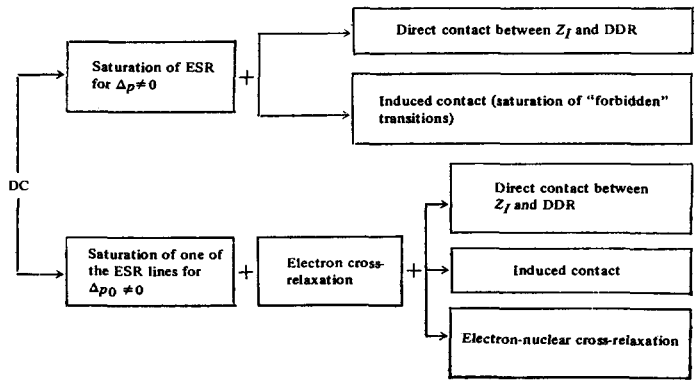

transforms into DC during electron cross-relaxation between spins S_1 and S_2.

In conclusion, we list the main features of the DC mechanism:

1. The reason for the nuclear polarization is the thermal contact between the nuclei and DDR, the temperature of which is reduced by the saturation of the electron transitions subject to $\Delta_p \neq 0$ and (or) the effective electron cross-relaxation.

2. The result of DC is the establishment of the equation $\beta_I = \beta_d$ and is independent of the path by which this equality has been reached.

3. The maximum achievable nuclear polarization is of the order of $p^0\omega_S/2\omega_d$, i.e., it is proportional to γ_I.

4. The DC mechanism can be looked upon as a generalization of the solid effect and of the electron-nuclear cross-relaxation to the case where DDR additionally participates in thermal mixing.

2. DNP IN SYSTEMS WITH AN INHOMOGENEOUSLY BROADENED ESR LINE

A. Inhomogeneous broadening

Inhomogeneous broadening of ESR lines, connected with the local distortions of the internal crystal field, hyperfine interactions between spins S and the nuclei of their own or the nearest-neighbor atoms, and so on, is usually important in real crystals with paramagnetic impurity concentrations $n_S \lesssim 10^{19}$ cm^{-3}.

Rigorous analysis of the dynamics of the spin system under the conditions of inhomogeneous broadening is a complicated problem which is usually simplified[47] by dividing the inhomogeneous line into uniform "spin packets" of equal width ξ, each of which is associated with a set of n_S^j "identical" spins S_j with Larmor frequency $\omega_j (\sum n_S^j = n_S)$.

If $G(\omega - \omega_0)$ is the shape function for the entire inhomogeneous line (ω_0 is the frequency at the center of gravity) and $\int_{-\infty}^{\infty} G(\omega - \omega_0) d\omega = 1$, it is clear that $n_S^j = \xi G(\Delta_j) n_S$, where $\Delta_j = \omega_j - \omega_0$ and it is assumed that the total width of the inhomogeneous line is $\delta_S \sim [G(0)]^{-1} \gg \xi$.

When the saturating high-frequency magnetic field of frequency ω_p is applied to the specimen, then, according to this model, only the spins S_i with Larmor frequency $\omega_i = \omega_p$ are directly subjected to this field, and the influence of the pump on the remaining line (if we ignore some overlap between the tails of neighboring packets) is achieved through cross-relaxation. The inclusion of the latter leads to the appearance of the so-called spectral diffusion[47-49] of electron polarization $P_j(\omega_j)$. The effective characteristic diffusion length (in frequency space) is $\Delta_D = \sqrt{\tau_{Si} D_\omega}$, where D_ω is the spectral diffusion coefficient which can be expressed[48,49] in terms of the probability w_{CR}. It is clear that Δ_D increases with increasing n_S and decreasing T_0.

If electron spin-spin interactions are stronger than the spin-lattice interactions, then, as in the case of homogeneous broadening, we must introduce DDR with its own temperature, and there is every reason to suppose[49] that it should be common to all the spins S.

We now proceed to analyze DNP, and again consider in succession SE, ENCR, and DC, assuming that the influence of inhomogeneous broadening of the ESR line is appreciable, i.e., $\bar{\delta}_S > \omega_I$.

B. Solid effect in an inhomogeneous line

Consider, as usual, the ideal SE, so that the allowed and "forbidden" transitions do not overlap for a given packet ($\xi \ll \omega_I$) and, moreover, cross-relaxation within the frequency interval ω_I is negligible ($\Delta_D \ll \omega_I$). The high-frequency field of frequency ω_p will then simultaneously produce the allowed transition for the i-th packet and the forbidden transitions with opposite signs for packets u and v with frequencies $\omega_u = \omega_i + \omega_I$ and $\omega_v = \omega_i - \omega_I$.

In the uniform-polarization model (see Fig. 2c), packets u and v compete with one another, producing polarization fluxes of different sign, whereas all the other packets play a passive role, facilitating leakage. If we now transform to the rotating coordinate frame by the usual recipe, we again obtain the thermal mixing equation, this time between the Zeeman subsystems of packets u and v in the rotating frame (Z_u^* and Z_v^*) with reciprocal temperatures $\beta_u^* = \beta_u \omega_u/\omega_I$ and $\beta_v^* = \beta_v \omega_v/\omega_I$ and the nuclear subsystem Z_I, where the time τ_{fI} is defined, of course, with account being taken of the influence of all the "idling" packets.

As a result, the thermal balance equation for $s^{\pm} \gg 1$ immediately yields

$$E^{\infty} \approx \frac{\omega_0 (G^+ - G^-)}{\omega_I (G^+ + G^-)(1 + f_{eff})}, \tag{2.1}$$

where $G^{\pm} = G(\Delta_i \pm \omega_I)$ and $f_{eff} = f n_S / (n_S^u + n_S^v)$.

The appearance of f_{eff} in (2.1) in place of f reflects the fact that only the small fraction $(n_S^u + n_S^v)/n_S$ of all the spins S participates in DNP.

Both (2.1) and other more detailed formulas for this case, which include the dependence of β_I and τ_ρ on $s^{\pm}$, are given in the literature.[20,37 54]

Thus, simultaneous saturation of "forbidden" transitions of packets u and v will reduce E^{∞} as compared with the ideal SE, but it is clear from (2.1) that this effect is not catastrophic, provided the wings of the inhomogeneous line fall off sufficiently rapidly ($G^{\pm} \ll G^-$). We note that, for a Gaussian line shape, E^{∞} may reach 80% of its ideal value[37,50] $\pm\gamma_S/\gamma_I$.

In the case of isolated spheres of influence with equal sphere volumes (see Fig. 2a), the result is completely different.[6] Here, the high polarization of the nuclei appears only in a negligible part of the specimen, and the spheres of influence of the "idling packet" have $p_J = p^0$. As a result, (1.11) yields

$$\bar{p}_{st} = p^0 \frac{\omega_{0S}^{\xi} (G^+ - G^-)}{\omega_I}, \tag{2.2}$$

i.e., the polarization is proportional not to the relative [as in (2.1)] but to the absolute difference between n_S^u and n_S^v. Since $\xi \ll \omega_I$, (2.2) predicts a substantially smaller DNP effect. If, in addition, $\omega_I \ll \bar{\delta}_S$, then $\bar{p}_{st} \propto dG/d\omega$, and hence this is often referred to as differential SE. Finally, in the model shown in Fig. 2b, the result can easily be obtained with the aid of (1.12) generalized to spin packets in an inhomogeneous line.[20b]

We note that the transition from isolated spheres of influence to uniform polarization can be achieved artificially if the pump frequency ω_p is varied sufficiently rapidly[51,52] with amplitude $\delta\omega \sim \omega_I$. This will saturate the forbidden transitions for all the packets within the frequency interval $\delta\omega$ which, in turn, will lead to the equalization of the nuclear polarizations in their spheres of influence and to an increase in E^{∞} due to the transition from (2.2) to (2.1). An analogous effect is expected when the electron spins "hop over" from one packet to another, for example, during fluctuations in the hyperfine local fields produced by nuclear spin flips in the immediate environment.[53]

C. ENCR in an inhomogeneous line

We now consider the situation where a high-frequency field induces only allowed transitions at the frequency $\omega_p = \omega_I$ but there is also efficient ENCR between any two spin packets m, n whose frequencies satisfy the condition

$$\omega_m - \omega_n = \pm\omega_I. \tag{2.3}$$

We begin with the uniform polarization model. It follows from sub-sec. E of Sec. 1 that, in this case, ENCR leads to

$$P_m - P_n = \mp p \tag{2.4}$$

for any pair of packets related by (2.3).

In particular, if the i-th packet experiences saturation, then successive application of (2.4) to pairs of packets with frequencies $\omega_i + \omega_I$, $\omega_i \pm 2\omega_I$, and so on, leads to the segregation from the inhomogeneous line of a "chain" of spin packets (Fig. 8) with frequencies $\omega_j = \omega_i \pm k\omega_I$ and polarizations

$$P_j = P_i \mp kp \qquad (k = 1, 2, \ldots). \tag{2.5}$$

To determine p, we treat the segregated "chain" in the same way as in sub-sec. E of Sec. 1, i.e., we subdivide the Zeeman energy of all its packets $\hat{\mathcal{H}}'_S$ into the resultant energy (Σ')

$$\hat{\mathcal{H}}'_{\Sigma} = \hbar\omega'_0 \sum_{j=1}^{R} \hat{S}_j^z,$$

where $R \approx \bar{\delta}_S/\omega_I$ is the number of packets in the chain and ω'_0 is the frequency at the center of gravity, and the difference energy (Δ') which is given by a linear combination of the quantities

$$\hat{\mathcal{H}}'_{\Delta mn} = (m - n)\omega_I \left(\frac{\hat{S}_m^z}{n_S^m} - \frac{\hat{S}_n^z}{n_S^n} \right). \tag{2.6}$$

As in the case of two ESR lines, the ENCR process involves the participation of only the Δ'-subsystem, all the eigenfrequencies of which are equal to or are multiples of ω_I, so that the result of ENCR should be the thermal mixing of this subsystem with Z_I. Transforming, as usual, to the rotating coordinate frame, we arrive at a thermal contact scheme for the subsystems Δ', Z_I, and $(\Sigma')^*$, which is analogous to that shown in Fig. 4. Next, taking into account the fact that ENCR couples nuclear spins with the subsystem Δ'' as well, and the latter system is formed by analogy with (2.6) from pairs of "idling" packets that were not members of the segregated "chain" used above, and using the thermal equation of the form of (1.18) and (1.22), we finally obtain

$$E^{\infty} = -\frac{\Delta'_{p0}\omega'_0}{(\Delta'_{p0})^2 + \alpha^{-1}(M_2 + f\omega_I^2)}, \tag{2.7}$$

where $\Delta'_{p0} = \omega_p - \omega'_0$, M_2 is the second moment of the entire inhomogeneous line, $\alpha = n'_S/n_S \approx \xi/\omega_I$, n'_S is the number of spins in the segregated "chain," and the factor f takes into account only the leakage due to nuclear relaxation with time τ_{1I}, which is unrelated to ENCR. In accordance with (2.7), the maximum DNP effect is achieved for $(\Delta'_{p0})^{max} = \pm\sqrt{(M_2 + f\omega_I^2)/\alpha}$, where $|E_{max}| = \omega_0/2\,|(\Delta'_{p0})^{max}| \propto \sqrt{\alpha}$.

We now consider the model of isolated spheres of influence. It is readily verified that, in this case (for

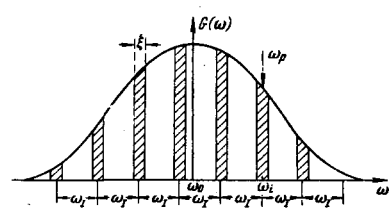

FIG. 8. Illustration of ENCR in an inhomogenous line: spin packets forming a segregated "chain" (see text) are shown shaded.

equal volume spheres),

$$\bar{p}_{st} = -\alpha p^0 \frac{\Delta'_{p0}\omega'_0}{(\Delta'_{p0})^2 + M'_2 + f\omega_I^2},$$

from which it is clear that the gain in p_{max} as compared with uniform polarization is roughly by a factor of $\sqrt{\alpha}$.

The above formulas, based as they are on the thermal mixing model, cannot, of course, give us p_{st} as a function of the pump and ENCR probabilities between the different packets. This requires the application of different approximate methods, for example, the solution of the set of equations for P_j without taking the nuclei into account. The resulting solution is then substituted[33] into the equation for p, or the analysis is confined to ENCR for only three spin packets with frequencies ω_i and $\omega_i \pm \omega_I$, and so on.

D. DC mechanisms in the case of inhomogeneous broadening

As the concentration of the spins S increases and the temperature decreases, there is an increase in the contribution of spectral diffusion and DDR, and the DC mechanism begins to operate. An analysis of this effect under the conditions of inhomogeneous broadening of ESR lines can be found in the literature.[10,16,37,39,41,54,55]

We assume, to begin with, that diffusion is effective throughout the line profile, i.e., $\Delta_D \gtrsim \delta_S$. To reduce this effect to thermal mixing, we again segregate the Σ-subsystem, $\hat{\mathcal{H}}_\Sigma = \hbar\omega_0 \sum_j S_j^z$, which does not participate in cross-relaxation, and write the remainder $\hat{\mathcal{H}}_\Delta = \hat{\mathcal{H}}_S - \hat{\mathcal{H}}_\Sigma$ in the form of a set of "difference" subsystems Δ_j, each of which can be given a reciprocal temperature $\beta_{\Delta j}$ just as in sub-sec. E of Sec. 1. Cross-relaxation leads to thermal contact between all the Δ_j subsystems, and DDR and saturation at frequency $\omega_p = \omega_0 + \Delta_{p0}$ mixes them with the cold subsystem Σ^* (in the rotating frame).[39,56] The situation here is analogous to the case of electron-nuclear cross-relaxation (sub-sec. C), except that the nuclei are now replaced by the DDR which has a continuous spectrum and, therefore, takes all the spin packets into a "common pot" rather than some segregated "chain." It is readily seen that this result should also ensue without spectral diffusion provided the overlap of the wings of all the spin packets, which leads to the simultaneous saturation of each of them (in the wing) by the high-frequency field, is taken into account.[56]

Insofar as the transfer of low temperature from DDR to the nuclei is concerned, we again encounter the same mechanisms as in the absence of inhomogeneous broadening: direct and induced contacts between Z_I and DDR, combination of pure electron cross-relaxation and ENCR, and so on (see sub-sec. F, Sec. 1). Thus, each of the DNP mechanisms discussed above leads, under the conditions of effective spectral diffusion, to thermal mixing of the following subsystems: Σ^*, all the Δ_j, DDR, and Z_i (Fig. 7). The "heat capacity" of the Δ-subsystem is $c_\Delta = \sum_j c_{\Delta j} = \hbar^2 M_2 n_S S(S+1)/3k$, so that the result of the mixing process is described by (1.27), provided M_2 and Δ_{p0} are suitably generalized. It is clear from a comparison of (1.27) with (2.7) that, when $\alpha \ll 1$, the DC mechanism turns out to be more advantageous than ENCR.

We note that the application of the principle of thermal mixing does not, in general, necessitate the subdivision of the inhomogeneous line into spin packets. It is, in fact, sufficient to assume only that internal processes establish a state of quasiequilibrium in the so-called "reservoir of local fields" with Hamiltonian $\hat{\mathcal{H}}_L = \hbar \sum_j \Delta_j \hat{S}_j^z + (\hat{\mathcal{H}}^0_{SS})'$, where j labels all the electron spins of the specimen and $(\hat{\mathcal{H}}^0_{SS})$ represents the component of $\hat{\mathcal{H}}_{SS}$ that commutes with $\hat{\mathcal{H}}_\Sigma$.[57] The result predicted on the basis of this more general model is practically indistinguishable from (1.27).

If spectral diffusion does not encompass the entire ESR line, saturation affects only a fraction of the spin packets, and a so-called "burnt-out hole" with center at ω_i and width Δ_D is produced.[47,48] The thermal mixing model can then be applied only to the hole produced in this way, and the remaining ("idle") packets are taken into account in the same way as in the analysis of ENCR (see above). This case has been analyzed in detail (using a different approach) by Buishvili *et al.*[49,54]

Inhomogeneous ESR line broadening leads to an appreciable increase[44,58,59] in the correlation time τ_S and, consequently, to a reduction in the direct contact between Z_I and DDR (see Sub-sec. F, Sec. 1).[5)] However, this has no effect on the other channel of coupling between Z_I and DDR, which is due to the simultaneous saturation of allowed and forbidden transitions so that, in the case of strong inhomogeneous broadening, one expects the gradual transition from SE to DC as the strength of the radiofrequency field increases.[10]

Let us now summarize. We have verified that inhomogeneous broadening of ESR lines leads to a reduction in the maximum achievable nuclear polarization for any DNP mechanism. The most favorable case of "pure" SE combined with uniform spatial polarization of nuclei leads to a substantial deterioration in the results for both ENCR and SE. Spectral diffusion gives rise to an increase in the fraction of active electron spins but, at the same time, produces a transition from SE to DC, which is accompanied by a reduction in nuclear polarization. Finally, when strong spectral diffusion takes place, the inhomogeneous line behaves in the same wav as a homogeneous line of width $\tilde{\delta}_S$.

E. Reaction of DNP on electron polarization

In experimental studies and practical applications of DNP, one frequently has to decide which of the above mechanisms predominates. When the ESR linewidth is less than ω_I, there is no real problem but, if there is strong inhomogeneous broadening, it is clear from the foregoing that there are no clear differences between SE, ENCR, and DC mechanisms. When this is so, useful information can be obtained by analyzing the distribution of stationary electron polarization within the limits of the profile of the inhomogeneous ESR line (to determine this distribution, one must use a second high-frequency field which saturates the electron spin system

[5)] See *footnote*[3)].

and serves only as an indicator of ESR absorption).

We begin, as usual, with the pure SE mechanism and assume that the high-frequency field of frequency $\omega_p = \omega_i$ produces strong saturation of the "forbidden" transitions of different signs for packets u and v with frequencies $\omega_i \pm \omega_I$. If the uniform polarization model is valid, the quantity p_{st} is constant throughout the specimen and, consequently, it follows from (1.5) that $P_u = -p_{st}$, $P_v = +p_{st}$, where p_{st} is given by (1.5) and, of course, does not reach the limiting value $\pm P^0$.

The distribution of electron polarization is then as illustrated in Fig. 9a, whilst Fig. 9b shows the shape of the induced signal due to ESR absorption, which differs from $P(\omega)$ only by the presence of the factor $G(\omega - \omega_0)$. It is clear that the ESR line should exhibit valleys on either side of the saturated i-th packet, and absorption at frequencies corresponding to large separation from ω_0 should be negative, i.e., we have stimulated emission or the "maser effect."

A different situation obtains in the model based on isolated spheres of influence. According to (1.5), the stationary polarization of the nuclei belonging to the spheres of influence of packet v is, in this case, given by $p_v = P_v = P^0/(1+f_v)$, and, correspondingly, for packet u we have $p_u = -P_u = -P^0/(1+f_u)$, where f_v, f_u are the leakage factors in the corresponding spheres. Thus, P_u and P_v now turn out to have the same sign, and are not very different from P^0 for f_u, $f_v \ll 1$ (Fig. 10).

If we use (2.5) together with considerations similar to those used above, we can readily obtain the stationary distribution $P(\omega_j)$ for the ENCR mechanism (Fig. 11). The polarization of all the packets satisfying (2.5) and belonging to the segregated "chain" satisfies a straight-line equation with slope $-p_{st}/\omega_I$ and intercept $\omega = \omega_p$ on the abscissa axis. This result is qualitatively the same for homogeneous polarization and isolated spheres of influence: the only difference lies in the magnitude of p_{st}. Under the conditions of ENCR, the other packets are also related in pairs by (2.3) and (2.4), so that, in the uniform polarization model, in which $p_{st} = \text{const}$ throughout the specimen, their polarizations will also satisfy linear relations with the same slope but different intercepts (Fig. 11).

If, on the other hand, the model of isolated spheres of influence is valid, $p_{st} = p^0$ in the spheres of influence of

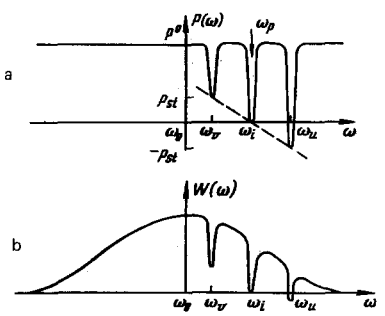

FIG. 9. Distribution of electron polarization over an inhomogenous ESR line (a) and ESR absorption signal shape (b) in the case of the solid effect using the inhomogenous polarization model.

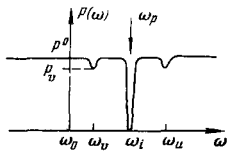

FIG. 10. Same as Fig. 9 (a) but for the model of isolated spheres of influence.

the "idle" packet, and the polarizations will not depart from P^0 (broken line in Fig. 11).

Finally, in the DC mechanism due to effective spectral diffusion throughout the inhomogeneous line (see sub-sec. B), we have equalization of the reciprocal temperatures β_L^*, β_d, β_I and all the $\beta_{\Delta j}$. It is readily verified that, for any j,

$$\beta_j^* = -\frac{\beta_j \omega_j}{\omega_j - \omega_p} = \beta_I,$$

from which it follows that the distribution of electron polarization over the inhomogeneous lines is described by the straight line $P(\omega) = -p_{st}(\omega - \omega_p)/\omega_I$ (Fig. 12). It is well known that this picture is characteristic of homogeneous lines with dipole broadening.[41,60]

In intermediate cases, when $\Delta_D \sim \omega_I$, the graphs of Figs. 9–12 are no longer entirely meaningful, and additional studies are necessary to elucidate the DNP mechanism (see below, sub-sec. A, Sec. 4).

Apart from the observation of $P(\omega)$ with the aid of a weak inducing high-frequency signal, there is another method of monitoring electron spins, namely, direct measurement of absorption of the high-frequency pump field at the frequency ω_p. In this case, nuclear polarization ensures that this absorption increases when an additional high-frequency field of frequency ω_I is applied to the specimen and saturates the nuclear Zeeman subsystem. The reason for this effect, which is called "distant ENDOR"[61] (electron nuclear double resonance on distant nuclei), is that saturation, i.e., the forced depolarization of the nuclei, is equivalent to an increase in the leakage factor f which, in its turn, moves the electron spin system away from the saturated state. Detailed analysis of this phenomenon for different DNP mechanisms can be found in the literature.[6,61-64]

3. DNP AT VERY LOW TEMPERATURES

So far, we have used the "high-temperature approximation" and confined our attention to the linear terms in the expansion for $\exp(\hbar\omega/2kT)$, i.e., we have assumed that p, $P \ll 1$. This, however, becomes incor-

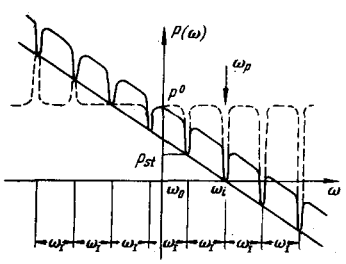

FIG. 11. Same as Fig. 9 (a) but for the ENCR mechanism: solid line—uniform polarization model, broken line—isolated spheres of influence, inclined straight line—the function $P(\omega) = -p_{st}(\omega - \omega_p)/\omega_I$.

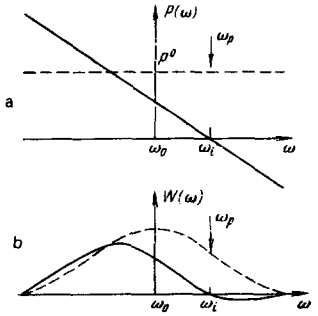

FIG. 12. Same as Fig. 9 but for the DC mechanism: the slope of the straight line in (a) is the same as in Fig. 11.

rect at very low temperatures and in sufficiently strong magnetic fields, i.e., under the conditions that are of maximum interest from the point of view of high degree of nuclear polarization (as an example, we note that $\hbar\omega_S/2kT_0 \approx 1$ for $\omega_S/2\pi = 70$ GHz and $T_0 = 1.5°$K). When the high-temperature approximation is no longer valid, the above results must be corrected in three different ways.

a) The first category of corrections involves direct allowance for the nonlinear dependence of polarization on temperature. The SE and ENCR equations given by (1.3) and (1.20) are formally unaltered except that the time τ_{Il}, due to the forbidden relaxation transitions, is now related to τ_{Sl} by [6,65]

$$\tau_{Il}^{-1} = \sigma\tau_{Sl}^{-1}(1 - PP_0), \tag{3.1}$$

so that (1.3) and (1.20) become nonlinear and the solution no longer has a simple and physically clear form.[22] Nevertheless, the main tendency of SE and ENCR represented by the expressions $p \to \pm P$ and $p \to \pm(P_1 - P_2)$ remains in force.

If "extraneous" relaxation of nuclei can be neglected, we can replace P in (3.1) by P^0 and obtain

$$\tau_{Il}^{-1} = \sigma\tau_{Sl}^{-1}\,\mathrm{sech}^2\frac{\hbar\omega_S}{2kT_0}.$$

We can then use (1.5), (1.22), and so on, remembering, however, the dependence of the factor f on P^0. An important consequence of this correction is the sharply reduced contribution of the deleterious effect of extraneous paramagnetic impurities for $P^0 \to 1$ (this is the so-called *"freezing out" of leakage*[22]).

Much more serious complications arise in the case of the DC mechanism. The point is that, when $\hbar\omega_S \gtrsim kT_S$, the subsystems Z_S^* and DDR can no longer be regarded as statistically independent because each electron spin flip affects the mean energy of DDR. This means that (1.23) is fundamentally incorrect, but cannot destroy the idea of thermal mixing in the rotating frame because the statistical independence of Z_S^* and DDR is not essential for the establishment of a common temperature of the combined (Z_S^* + DDR) system. However, the old recipe cannot be used without modification because the "heat capacities" introduced previously are now functions of temperature and the thermal balance equation must be written in the more general form

$$\frac{d}{dt}\Big(\sum_i \langle\hat{\mathcal{H}}_i\rangle\Big) = -\sum_i \tau_{il}^{-1}\big(\langle\hat{\mathcal{H}}_i\rangle - \langle\hat{\mathcal{H}}_i^0\rangle\big), \tag{3.2}$$

where i lables the subsystems participating in thermal mixing and $\langle\mathcal{H}_i^0\rangle$ is the value of $\langle\hat{\mathcal{H}}_i\rangle$ at the temperature of the lattice.

For the inhomogeneously broadened line with effective spectral diffusion and $\omega_d^2 \ll M_2$, Eq. (3.2) yields

$$\frac{1}{n_S}\sum_j n_S^j(\Delta_{p0} - \Delta_j)(P_j)_{st} + f\omega_{1I}p_{st} = \Delta_{p0}P_0, \tag{3.3}$$

where the stationary polarization of the j-th packet is

$$(P_j)_{st} = -\tanh\frac{\hbar(\Delta_j - \Delta_{p0})\beta_{st}^*}{2k}.$$

Thus, (3.3) is a transcendental equation for β_{st}^* and, consequently, $p_{st} = \mathrm{th}(\hbar\omega_I\beta_{st}^*/2k)$. It is clear that, in the high-temperature approximation, Eq. (3.3) directly leads to the previous formula given by (1.27). Equation (3.3) was first obtained by Borghini[39] (by a somewhat different procedure) and serves as the basis for DNP calculations at low temperatures.[40,66] Numerical analyses of this equation[66,67] have shown that the overall DNP picture is not very different from the high-temperature case, except that the detuning $|\Delta_{p0}^{max}|$ corresponding to $|p_{st}|$ increases monotonically with decreasing T_0. At the same time, $|p_{st}^{max}| \to 1$. It is important to note that the rate of direct contact between nuclei and DDR is proportional to $1 - P^2$ and, therefore, its efficiency at low temperatures may be substantially lower.[14]

When the DDR energy cannot be neglected in the thermal-balance equation (in particular, in the case of DC with a homogeneously broadened ESR line), the transcendental equation for β_{st}^* becomes more complicated,[14,68] but nothing qualitatively new is expected.

b) The other source of complication at low temperatures is the so-called "phonon bottle-neck" in electron spin-lattice relaxation. It is well known[69] that energy transfer from saturated electron spins to the thermostat (for example, a helium bath) is delayed because of the low specific heat of phonons "resonating" with the spins at frequencies within the band δ_S near ω_S. The result is that the effective temperature T_{ph} of these phonons increases relative to T_0, and the observed electron relaxation time rises to $\tau_{Sl} = (1 + \sigma')\tau_{Sl}$, where σ' is the "phonon-bottle-neck factor" determined by the ratio of the rates of relaxation of the "resonating" phonons to the spins S and to the bath, respectively. We note that, although this effect can arise only at sufficiently low temperatures, it is not necessarily connected with the breakdown of the "high-temperature" approximation (P, $p \ll 1$).

In the case of ideal SE, when only the "forbidden" transitions are saturated, the phonon bottle-neck has relatively little effect on DNP (the only effect is that τ_{Sl} is replaced by τ'_{Sl} in the leakage factor f[22]). If, on the other hand, allowed transitions are also saturated, and this happens in ENCR, DC, and in the case of strong inhomogeneous ESR line broadening, the negative role of phonon overheating is found to increase sharply.

In the more "liberal" model, it is assumed that pho-

nons are heated equally throughout the frequency band δ_S and the result of this is again that τ_{Sl} is replaced by τ'_{Sl} in (1.25) and (1.27).[70,71] Since, on the other hand, the time τ_{dl} does not increase under these conditions (the DDR heat capacity is too low for this), it follows that the maximum achievable nuclear polarization for $\sigma' \gg 1$ is reduced roughly by a factor of $\sqrt{\sigma'}$.

More dramatic consequences arise when the "overheated" phonons within the interval δ_S do not exchange energy among themselves (this is, of course, expected because inelastic scattering of phonons at low temperatures is usually negligible). In this situation, the frequency dependence of T_{ph} within the ESR line profile is determined by the departure of the $P(\omega)$ curve from equilibrium. Since, however, part of the ESR line is inverted in the DC mechanism (see Fig. 12), equilibrium between spins and phonons within this part of the spectrum can be achieved only for $T_{ph}<0$, which is not, of course, possible because the phonon spectrum is restricted at the top. As a result, the number of phonons within the narrow frequency band tends to increase rapidly (this is the "phonon avalanche") and T_{ph} rises[72,73] to a few thousand °K which, in turn, leads to a practically instantaneous increase in $|\beta_d^{-1}|$ and to the disappearance of DNP.

Fortunately, the phonon bottle-neck effect decreases with increasing $\tilde{\delta}_S$ (σ' is proportional to the number of spins S per unit spectrum interval), so that phonon overheating must usually be taken into account only for narrow ESR lines, when SE predominates and nothing catastrophic occurs.

c) Finally, the third feature that is characteristic for low temperatures consists of shifts and changes in the shape of the NMR and ESR lines, which are due to local fields of highly polarized electrons and nuclei. The basic features of these effects are reasonably well known.[6] From the practical point of view, the most important consequence is the violation of proportionality between the NMR signal amplitude and p, so that the entire area under the NMR absorption line must be taken into account if the latter quantity is to be determined. On the other hand, it has recently been suggested that these distortions of the NMR line shape may be used as a basis for a convenient and effective method of direct determination of p and a number of other parameters of the electron spin system, namely, the time τ_{Sl}, the concentration n_S, and the factor σ' (this is the so-called nuclear-electron double resonance–NEDOR[74,75]).

4. DNP EXPERIMENTS IN THE CASE OF ELECTRON-NUCLEAR DIPOLE INTERACTION

The enormous experimental material accumulated so far can be conveniently divided into two categories, namely, experiments designed to elucidate the DNP mechanisms and results of practical utility, for example, in nuclear physics.

A. Identification of the DNP mechanisms

As usual, we begin with the "ideal" SE. Here, the clearest illustration is provided by the well-known experiments on the polarization of protons in the water of crystallization of lanthanum-magnesium nitrate (LMN), $La_2Mg_3(NO_3)_{12} \cdot 24H_2O$, containing Nd^{3+} impurities.[65] Figure 13 shows a typical dependence of E_{st} on Δ_p, and it is clear that polarization maxima are achieved for $\Delta_p = \pm\omega_I$ (in this case, $H_0 = 19.5$ kOe, $T_0 = 4.2$ °K, $\nu_S \equiv \omega_S/2\pi = 74$ GHz, $\nu_I \equiv \omega_I/2\pi = 83$ MHz).

The particular feature of Nd^{3+}:LMN is the relatively narrow ESR line (about 23 MHz under these conditions), so that the "ideal" SE condition $\delta_S \ll \omega_I$ is readily satisfied.

At 4.2°K, the experimental data on DNP in this crystal, including the dependence of p and τ_p on s^+, are in good agreement with elementary theory[65,6] (see sub-sec. B, Sec. 1). However, certain discrepancies begin when the temperature is reduced to 1.4°K: despite the fact that $f \ll 1$, it is found that $p_{max} = 70\%$ and does not reach $|P^0| = 83\%$ in this case. Moreover, much more pump power is necessary than predicted by (1.4) to achieve maximum polarization. These features can be explained only by the presence of the phonon bottle-neck[22] (see Sec. 3) with $\sigma' \approx 500$.

It is worthwhile to note some results on SE in the case of inhomogeneously broadened ESR lines. In early work,[6] it was usually assumed that the model of equal-volume isolated spheres of influence could be used and the results were interpreted in accordance with (2.2). However, this tradition was abandoned in work[50,76] performed on yttrium ethyl sulfide crystals containing Er^{3+}. In these experiments, the enhancement of proton polarization was much greater than the amount predicted by (2.2), but was in good agreement with (2.1), indicating sufficiently rapid nuclear spin diffusion.

The formula given by (2.1) was also confirmed in DNP experiments with lithium fluoride[53] containing V_k centers ($T_0 = 80$°K, $\nu_S = 9.5$ GHz, $\tilde{\delta}_S/\gamma_S = 13$ Oe). In this case, however, the corresponding estimates are not in agreement with the fast spin diffusion model and a different explanation relaying on the inclusion of fluctuations in hyperfine local fields due to nuclear spins of ^{19}F had to be introduced (see sub-sec. B, Sec. 2). These "fluctuations" have also been produced artificially[51,52] by modulating the field H_0 at 10–100 kHz. This produced an increase in p_{max} for CaF_2 crystals containing atomic hydrogen impurities ($T_0 = 290$°K, $\nu_S = 9$ GHz,

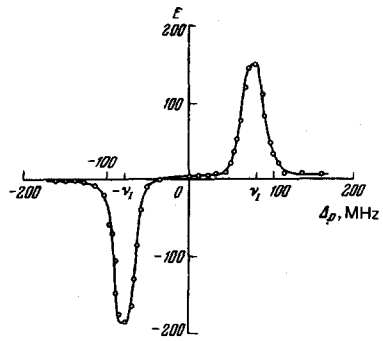

FIG. 13. Dependence of the enhancement of the polarization of protons E as a function of Δp in the LMN crystal with 1% of Nd^{3+} at 4.2 °K ($\nu_S = 74$ GHz, $H_0 = 19.5$ kOe).

$E_{max} = 190$)[51] and U^{3+} ions ($T_0 = 1.05$°K, $\nu_S = 70$ GHz, $p_{max} = 45\%$)[52] by a factor of 1.5–2.

The most interesting experiments on the DNP mechanism were performed in recent years and were concerned with the determination of the role of electron spin-spin interaction, i.e., ENCR and DC mechanisms. The idea of ENCR was first put forward in the course of the interpretation of DNP results on protons in irradiated polyethylene[13] (the experiments were performed for $H_0 = 3$ kOe and $T_0 = 1.6$–77°K). The simple model involving ENCR between packets in inhomogeneous lines provided a qualitative explanation of the observed "anomaly" (reduction in E_{max} and increase in Δ_p^{max} as T_0 decreases),[13,32] but it is now clear that complete agreement cannot be achieved without including DDR, the theory of which had not been developed at the time. The ENCR model without DDR and thermal mixing was subsequently used by Hwang and Hill[33] in the interpretation of DNP data on polystyrene containing some free radicals ($T_0 = 4.2$°K, $H_0 = 25$ kOe, $E_{max} = 40$),[77] polystyrene containing the DPPH radical ($T_0 = 1.6$–4.2°K, $H_0 = 3$ kOe, $E_{max} = 25$),[34] and so on. Agreement with theory was achieved by phenomenological fitting involving three parameters (the width of the "burnt-out" hole, the rate of spectral diffusion, and the saturation factor), but this was not, of course, very convincing. An interesting feature of these experiments was the reduction in Δ_p^{max} with increasing n_S. This effect might be explained[78] by the influence of exchange interactions between the spins S.

The poor agreement between theory and experiment was also characteristic of other DNP experiments performed at helium temperatures (for example, it was found that $p_{max} = 21.5\%$ for yttrium ethyl sulfate crystals containing Nd^{3+} at $T_0 = 2.1$°K and $\nu_S = 69.5$ GHz, whereas the theoretical value is 66%[79]). This was the situation until electron DDR was rigorously taken into account. Systematic experiments devoted to this problem were performed simultaneously and independently at two laboratories, one in the USSR and the other in Holland.

In the former, the experiments were performed with ^{27}Al nuclei ($I = 5/2$) in Al_2O_3 crystals containing Cr^{3+} (ruby) at $\nu_S = 9$ GHz, $T_0 = 1.8$–4.2°K.[80-82] The ESR spectrum of the chromium ion ($S = 3/2$) consists of everal lines. The cross-relaxation between these lines, combined with the saturation of one of them, was, in fact, used to cool the DDR (see sub-sec. F, Sec. 1). The result was an enhancement of the polarization of the ^{27}Al nuclei, whose magnitude was exactly in agreement with β_d/β_0 (Fig. 14).[6)]

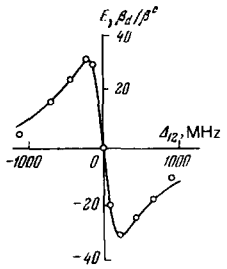

FIG. 14. Enhancement of polarization of ^{27}Al (E, open circles) and degree of DDR cooling (β_d/β_0, solid curve) as a function of the detuning Δ_{12} between the two ESR lines involved in the cross-relaxation (one of them is saturated by the high-frequency field)[82]. Al_2O_3 crystal with 0.03% of Cr^{3+}, $T_0 = 1.9$ °K, $H_0 = 3.3$ kOe.

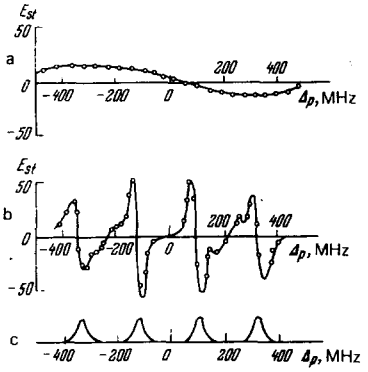

FIG. 15. Enhancement of polarization of protons E_{st} in a crystal of $ZnCs_2(SO_4)_2 \cdot 6H_2O$ with 0.5% of Cu^{2+} as a function of the detuning Δp of the high-frequency field relative to the center of gravity of the ESR spectrum ($H_0 = 3$ kOe)[91]: (a) $T_0 = 1.5$ °K, (b) $T_0 = 14$ °K, (c) ESR spectrum of the Cu^{2+} ion.

These results were the first direct experimental confirmation of the DC mechanism and, in particular, of the thermal mixing of the subsystems Δ, DDR, and Z_I. Measurements of nuclear spin-lattice relaxation in this material and a number of other experiments[83,84] have shown that this mixing also occurs in the absence of the high-frequency pump, i.e., it is due to the direct contact between DDR and Z_I. Subsequently, when a convenient method for direct determination of β_d from the dynamic longitudinal susceptibility signal became available,[85] this conclusion was confirmed by direct observations of a synchronous change in the temperatures β_I^{-1} and β_d^{-1} in different transient processes.[86,87] We note that both the functions $E(\Delta_p)$ and the absolute values of E_{max} and Δ_p^{max} reported in the literature[82] are in complete agreement with the DC theory. A comparable agreement can also be achieved for data obtained as a result of experiments with ruby[88] performed by other authors in higher fields ($\nu_S = 35$ GHz, $E_{max} = 360$).

Data have also been obtained[89] on DNP of ^{19}F in BaF_2 crystals containing Er^{3+} ($T_0 = 1.8$°K, $\nu_S = 9.5$ GHz). Since the Er^{3+} ion has a number of possible positions in the lattice of this crystal, the ESR spectrum consists of five lines, each of which has a number of lower-intensity satellites belonging to the hyperfine structure associated with the odd isotopes of erbium. The entire spectrum is connected with effective electron cross-relaxation, and it can be shown[89] that it can be looked upon as a single inhomogeneous "line." The saturation of the individual spectrum components (at the center of each of them) led to DNP of the fluorine and complete agreement between β_I and all the $\beta_{\Delta j}$, i.e., thermal mixing of Z_S^*, all the Δ_j, DDR, and Z_I^*, was observed (see sub-sec. D, Sec. 2).

[6)] ENCR made no contribution in this experiment because $\nu_I = 3.5$ MHz $\ll \Delta_{12}$.

Similar experiments were performed by the Dutch group who began[45,90,91] with LMN containing Nd^{3+} and Ce^{3+} but, in contrast to the other work,[62,65] these experiments were performed in low magnetic fields ($H_0 = 3.5$ kOe) for which $\delta_S \gtrsim \omega_I$. Very similar data were obtained for the two impurities, including the dependence of E and τ_p on Δ_p, n_S, and T_0 and the saturating power. In the first experiments in this series,[45,90] the DNP source was assumed to be only the induced contact between Z_I and DDR (see Sub-sec. E, Sec. 1), so that the experiment was in good agreement with theory only for sufficiently strong ESR saturation. A special experiment was subsequently performed and confirmed the presence of direct contact[92] and a more correct interpretation resolving all these difficulties was later given.[91]

The Dutch group also performed a major series of DNP experiments on crystals of the Tutton salts of zinc of the form $ZnX_2(SO_4)_2 \cdot 6H_2O$, where $X = NH_4$, K, Rb, Cs, Tl, containing Cu^{2+}.[93-95] The ESR spectrum of the latter contains four lines (hyperfine structure due to the nuclear spin of copper $I' = 3/2$) between which there is possible effective cross-relaxation just as in the case of Er^{3+}:BaF_2, described above. Similar proton DNP studies in conjunction with experiments on nuclear spin-lattice relaxation and DENR have completely confirmed the thermal mixing between Z_I and the combined subsystem Δ + DDR.

A very significant result was obtained for this material when the temperature T_0 was raised from 1.5 to 14°K (Fig. 15). In the first case, $\tau_S^{-1} \ll w_{CR}$, and the function $E_{st}(\Delta_p)$ is characteristic for the combined inhomogeneous ESR line under the conditions of effective spectral diffusion, whereas at 14°K, $\tau_S^{-1} \gg w_{CR}$, and each of the four components of the ESR spectrum provides its own independent contribution to DNP.[91]

Other methods of identifying the DNP mechanism were subsequently developed. Thus, experiments have been performed[96] with partially deuterized frozen butyl alcohol (the paramagnetic impurity was the porphyrexide radical) and the polarization of protons and deuterons was compared. The experimental data obtained at 0.5–1°K in fields of 25 and 50 kOe and for different detuning Δ_p have shown that, in all cases, there was accurate agreement between the Zeeman spin temperatures of both types of nucleus. This result is, of course, in complete agreement with the thermal mixing model, but is in conflict with the SE and ENCR models without DDR.

Comparison of the temperatures of different nuclei was subsequently carried out for deuterized ethylene glycol and propanediol containing CrV at $H_0 = 25$ kOe and $T_0 = 0.1$–0.5°K (the nuclei ^1H, ^2D, and ^{13}C),[97] and for LiF crystals containing paramagnetic F-centers under roughly the same conditions (the nuclei ^7Li and ^{19}F).[59,98] In both cases, nuclei of all types had the same temperature. It is interesting to note that if the NMR line of one nuclear type is saturated by the radiofrequency field after stationary polarization is reached then the temperature of the other (Fig. 16) tends to return to the common value with a characteristic time constant proportional to $1 - p^2$ when this field is turned off.

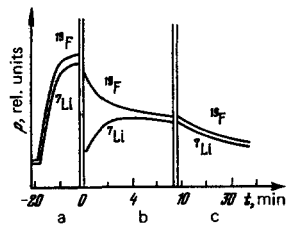

FIG. 16. Evolution of the polarization of the ^{19}F and ^7Li nuclei in LiF with F-centers at $T_0 = 0.74$ °K and $H_0 = 25$ kOe[98]: a—establishment of stationary polarization after the pump is turned on, b—thermal mixing after turning off the pump and instantaneous saturation of NMR of ^7Li (at $t = 0$), c—combined spin-lattice relaxation of ^{19}F and ^7Li.

Of course, comparison of the spin temperatures of different nuclei is not always possible in practice. A different method was proposed and used by Atsarkin *et al.*[99] to determine the DNP mechanism. This is based on the simultaneous application of two fields with somewhat different frequencies ω_p' and ω_p'' saturating an inhomogeneously broadened ESR line at different points on its profile. Without going into details, we note that for $\omega_p' - \omega_p'' = \pm k\omega_I$ ($k = 1$ for SE, and k is an integer for ENCR), there is a sharp reduction in p_{st}, whereas, for the DC mechanism, the second field does not have a resonance effect. In particular, this method was used to establish that the DC mechanism predominated in frozen ethyl glycol containing CrV at $H_0 = 13$ kOe and $T_0 = 1.8$°K ($E_{max} = 180$), when the central part of the ESR line was saturated, and was replaced by SE (or ENCR) in its distant wings. An analogous conclusion (although based on indirect evidence) was also reached by Wollan[76] in the case of DNP of hydrogen in yttrium ethyl sulfate crystals containing Er^{3+}.

A clear change in the DNP mechanism when Δ_p was increased has also been observed in a number of cases for which the "forbidden" transitions were spectrally resolved but the inequality $\omega_I > \delta_S$ was not very strong. A clear example is shown in Fig. 17, which gives the function $p(\Delta_p)$ for protons in partially deuterized m-xylene containing BDPA radicals at $H_0 = 25$ kOe and $T_0 = 0.5$°K ($\delta_S/2\pi = 20$ MHz, $\nu_I = 100$ MHz).[100] It is clear that the polarization maxima were observed both for $\Delta_p = \pm\omega_I > \delta_S$ (SE mechanism) and for smaller detunings within

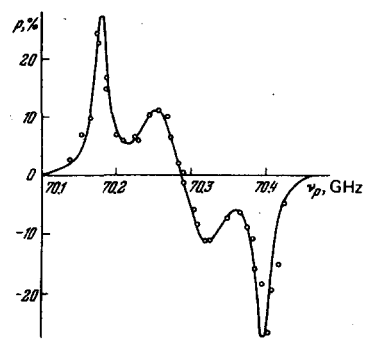

FIG. 17. Polarization p of protons in m-xylene with the BDPA radical as a function of pump frequency ($T_0 = 0.5$ °K, $H_0 = 25$ kOe)[100].

the ESR line profile (DC mechanism). It is interesting that this experiment provided evidence for additional maxima of p (not shown in Fig. 17) at $\Delta_p = \omega_S \pm 2\omega_I$ (this is the "double SE"). Results similar to those shown in Fig. 7 have also been reported elsewhere in the literature.[101,102]

Summarizing, we may conclude that the DC mechanism has been completely confirmed experimentally and, together with SE, forms the basis for a quantitative interpretation of DNP experiments. On the other hand, ENCR in its "pure" form, i.e., without electron cross-relaxation and DDR, has not as yet received equally convincing experimental support.

B. Production of high nuclear polarization and applications of DNP

The most important area of application of objects with a high degree of nuclear polarization is in the field of polarized targets, used in experiments on elementary-particle scattering.[2] First and foremost, such experiments require polarized protons and, therefore, most of the published results on high degree of polarization refer to hydrogen-containing materials.

The first material used in this field was LMN containing Nd^{3+} for which the following values were successively achieved: $p_{max} = 51\%$ ($\nu_S = 50$ GHz, $T_0 = 1.35$ °K), 72% ($\nu_S = 74$ GHz, $T_0 = 1.5$ °K), and, finally, 84% ($\nu_S = 70$ GHz, $T_0 = 1.12$ °K).[6,10] Roughly similar results were obtained for LMN containing dysprosium impurities at $T_0 = 1$ °K and $\nu_S = 126$ GHz.[103]

Despite the high value of p_{max}, LMN is not a very good material for polarized targets because the percentage of "free," i.e., unbonded to other nuclei, protons is too low in this medium (the concentration C_H of hydrogen by weight in LMN is only 3.1%). Search for materials with both high enough C_H and p_{max} has intensified in recent years. Many attempts have been made to obtain a high degree of polarization of protons in hydrogen-containing polymers, e.g., polystyrene or polyethylene containing paramagnetic centers produced by irradiation or by the introduction of stable free radicals.[6,10,77,104-106] However, none of them has been entirely successful although, in many cases, the condition $\delta_S < \omega_I$ was satisfied[77] and the "ideal" SE could have been expected. In polyethylene containing the TMPO radical, the reported result was $p_{max} = 50\%$ for $H_0 = 27$ kOe, but this required[107] the cooling of the specimen down to 0.1 °K by a mixture of ^3He and ^4He. Many other organic compounds containing free radicals were also found not to be promising in this respect.[108]

The long expected breakthrough occurred in 1969 when CERN and the French Center for Nuclear Studies at Saclary simultaneously succeeded in producing proton polarizations of 40–50% in frozen alcohols at 25 kOe and 1 °K.[109,110] One of these experiments[109] used ethylene glycol $(CH_2OH)_2$ containing CrV,[111] and the other[110] used butyl alcohol or butanol C_4H_9OH containing 5% water and an admixture of the prophyrexide radical. In both cases, the ESR line was inhomogeneously broadened and $\bar{\delta}_S$ was determined by the anisotropy of the electron g factor, and was proportional to H_0. It was found that $\bar{\delta} \approx 2\omega_I$ for fields in excess of 10 kOe. For ethyl glycol, $C_H = 9.7\%$, and the corresponding value for butanol was 13.5%. These and certain other frozen alcohols are at present the best materials for polarized targets. The corresponding results are summarized in Table II, which gives, for comparison, data for certain other media, including crystals.

It is clear from Table II that, in butanol, ethyl glycol and the more complex polyatomic alcohols, the magnitude of p_{max} increases with increasing H_0 and decreasing T_0. The record polarization achieved for $T_0 < 0.5$ °K is practically 100%. It has been shown[40] that this dependence of p_{max} on H_0/T_0 is in qualitative agreement with the DC model. We note particularly the result obtained for solid ammonia for which C_H approaches 17% (Table II). Unfortunately, the use of this medium as target material has been delayed for technical reasons involving difficulties in operating with NH_3 which is a gas at room temperature.

We note that a substantial DNP effect has not as yet been achieved in the "ideal" material such as orthohydrogen because of the rotation of the H_2 molecule which reduces[6] the time τ_{1l}. On the other hand, the static method (at $T_0 = 23$ mK, $H_0 = 100$ kOe) has been used for solid HD with a small impurity of ortho-H_2 to produce proton polarization[127] of up to 40%.

Technological difficulties connected with the removal of heat are common to all these experiments. Although the pump power necessary for DNP decreases sharply with decreasing T_0 (for butanol, it is 100 mW/cm^3 at 1 °K and only 2 mW/cm^3 at 0.5 °K[128]), the heating of the specimen can be avoided only by breaking it down into particles with linear dimensions of about 1 mm. Since most of the media listed in Table II are liquids at 300 °K, they must be sprayed into liquid nitrogen and the resulting particles have to be collected, which is, of course, rather inconvenient. A search is therefore in progress for suitable materials that are solid at room temperatures. These include pinacol, 1,8-octanediol (Table II), and some of the higher double alcohols in the same series, but p_{max} is found to decrease with increasing molecular weight.[117,118] Hopeful results have also been obtained for 1,2-cyclohexanediol containing CrV.[129]

The other approach is the search for crystals containing more hydrogen than LMN. Reasonable results have been obtained[125] for $NH_4Al(SO_4)_2 \cdot 12H_2O$ ($C_H = 6.18\%$) containing Cr^{3+}. The ESR lines of these crystals are narrow enough to ensure that SE predominates. The LiH crystals are more promising still (see Table II).

Since the time τ_{1l} is much longer at low temperatures, approaching many hours or even days for $T_0 \lesssim 0.5$ °K, we have the possibility of being able to turn off the pump source after the completion of DNP, and transferring the specimen to a weaker magnetic field, which makes scattering experiments much easier. Such "frozen" targets have already been used[107,123,130] and appear to be the most promising.

TABLE II.

Matrix	Paramagnetic impurity	H_0, (kOe)	T_0, °K	p_{max}, %	C_H, %	Reference
Ethylene glycol	Complex with CrV	25	1.4	40	9.7	[112]
		25	1.14	42—50		[109,113]
		25	0.5	80		[114]
		25	0.38	97*)		[97]
		47.5	1.1	80		[68]
1,2-propandiol	"	25	1.0	50	10.6	[115]
		25	0.55	83		[115]
		25	0.48	92		[115]
		25	0.37	98		[116]
Pinacone	"	25	0.5	60—70	11.9	[104]
1,8-octandiol	Complex of ethylene glycol with CrV	25	1.0	30	12.3	[117,118]
Butanol with 5% of water	Porphyrexide radical	25	1.4	27	13.5	[119]
		25	1.0	37—45		[110,113,120]
		25	0.5	67		[119]
		50	1.2	65		[121]
		50	1.0	73—80		[121, 122]
Glycerin-water mixture (1:1)	"	25	1.2	50	9.9	[123]
		25	0.5	60		[123]
		48	1.2	60		[123]
		48	0.5	70		[123]
Solid ammonia + 10% of glycerin	Complex of glycerin with CrV	25	1.0	42	16.7	[124]
Polyethylene	TMPO radical	27	0.1	50	14.3	[107]
Alum	Cr^{3+}	19.5	1.0	50	6.2	[125]
LiH	*F*-centers	50	0.6	50	12.5	[126]

*Partially deuterized sample.

We must also recall that values $p_{max} \approx 95\%$ have been obtained only for $H_0/T_0 \geq 60$ kOe/deg, whereas $|P^0|$ approaches 95% even for $H_0/T_0 \approx 30$ kOe/deg. Since $p_{max} = \pm P$ for the ideal SE, it is possible, at least in principle, to develop polarized targets capable of operating in lower fields and (or) higher temperatures, which again would substantially faciliate their application. This aim will be reached after further searches for suitable materials.

Polarized deuterium nuclei ($I = 1$, $\gamma_I/2\pi = 653.5$ Hz/Oe) have also begun to be used in scattering experiments. The best DNP results obtained so far are those for frozen alcohols, namely, deuterized ethylene glycol and propanediol containing CrV ($p_{max} = 40\%$ at 0.38 °K and 25 kOe[97,129]) and deuterized butanol containing porphyrexide (27%) at 1 °K and 50 kOe; 2% at 0.5 °K and 25 kOe[128,131]). Experiments on the transfer of polarization from protons to deuterons in solid HD are also interesting.[132]

Apart from their application to polarized targets, objects with nuclear polarization approaching unity are also of independent interest. They can be used to observe many unique phenomena in spin dynamics, including the most striking, namely, nuclear ferro- and antiferromagnetism.[3,133-137] We shall not pause to consider these very interesting experiments but merely emphasize that they have been possible only as a result of successes in the area of DNP techniques.

We also note the application of DNP to the development of neutron polarizers and to the study of the so-called nuclear pseudomagnetism.[138]

Less exotic applications of DNP include amplification of weak NMR signals due to low-abundance isotopes or nuclei with small values of γ_I. Examples are experiments with ruby (in which NMR due to ^{17}O has been observed[139]) and rutile (TiO_2 containing Cr^{3+} for which NMR due to ^{17}O, ^{47}Ti, and ^{49}Ti has been observed[140]).

A separate group consists of interesting experiments with $I > 1/2$ nuclei in which DNP was observed during saturation of the inhomogeneous ESR line exactly at its center.[88,141-144] This effect has been explained within the framework of the SE mechanism and is used to determine the sing of the nuclear quadrupole splitting constant[88,142] and internal stresses in crystals.[145-147]

Finally, we note the DNP experiment performed with acoustic pumps[148] and the original idea of using DNP to control future gamma lasers.[149]

5. OTHER DNP METHODS AND MECHANISMS

Other methods for DNP in solid dielectrics have not reached the same stage of development as those described above, and we shall therefore only briefly describe them here.

The Overhauser effect[1,6] differs from SE by the fact that an allowed ESR transition is subjected to high-frequency saturation (strictly in resonance), and nuclear polarization arises because electron-nuclear relaxation transitions with different signs have different probabilities. If one of them is zero, maximum enhancement of nuclear polarization can amount to $|\gamma_S/\gamma_I|$ but, for various reasons, this limiting value cannot be achieved.

The conditions necessary for the realization of this effect are satisfied only in the case of sufficiently rapid mutual mixing of spins S and I in space and, therefore, the effect is mostly seen in liquids, metals and semiconductors. Nevertheless, the Overhauser effect is possible in solid dielectrics when the spins S are coupled by a strong exchange interaction which, in this case, turns out to be equivalent to spin hops in space. DNP data in such materials are given, for example, by Jeffries[6] and turn out to be useful for estimating the nature and strength of exchange interactions.

For media occupying intermediate positions between liquid and solid states, and for diluted compounds with strong exchange, both the Overhauser and the solid effects are frequently observed. The function $p(\Delta_p)$ in such cases is the superposition of two curves, one symmetric and one antisymmetric relative to ω_S. As the temperature is reduced, the viscosity is increased, the concentration of centers undergoing exchange interaction is increased, and the magnetic field is increased, one observes a continuous transition from the Overhauser effect to SE.[18,150,151] The general theory of both DNP mechanisms, based on a unified approach to these phenomena, is given by Panon *et al.*[152]

A phenomenon similar to the Overhauser effect has also been observed during the motion of triplet $S = 1$ excitons in crystals under thermal[153] or electromagnetic[154] excitation. The high-frequency pump was not required in the latter case because nonequilibrium population of the electronic magnetic sublevels was produced as a consequence of selection rules when the triplet excitons were formed under illumination by light.

There are also other methods for the optical polarization of nuclei,[155] but most of them align only nuclei of impurity paramagnetic centers (occasionally, cross-relaxation can be used to transfer this polarization to the nuclei of the matrix: for example, in CaF_2 crystals containing Tm^{2+}, the optical polarization of ^{169}Tm at 1.9 °K was found to lead to an enhancement of the polarization of ^{19}F nuclei by a factor of 30[156]). An important exception is provided by molecular crystals (naphthalene, fluorine, and certain others) with small impurities of "foreign" molecules (anthracene, and so on) in which exposure to unpolarized near-ultraviolet radiation produces a substantial enhancement in proton polarization.[154,157-159] Thus, $E = 30\,000$ (!) has been achieved[158] in fluorine crystals containing acridine at $T_0 = 300$ °K and $H_0 \approx 100$ Oe, but the absolute value of p was then only 0.1%. The mechanism responsible for optical polarization of the nuclei in these materials is connected with the selective population and deexcitation of electron-nuclear magnetic sublevels in the excited triplet states of the impurity.[157]

The first attempt to increase the absolute value of p by this method[160] by performing the experiment at 4.2 °K was not successful, although it was useful from the point of view of achieving better understanding of the optical polarization mechanism. Nevertheless, estimates have shown that this aim can, in principle, be achieved by suitably choosing the working medium. If this is indeed the case, we have here the possibility of producing high proton polarization at moderate temperatures and in low magnetic fields, which is of undoubted interest for the technology of polarized targets and other applications.

Finally, there is a number of DNP methods using the relatively strong hyperfine interaction between electron spins and nuclei in the impurity paramagnetic centers or atoms belonging to their immediate environment.[6] However, these methods do not produce polarization of the host lattice.

CONCLUSIONS

DNP theory and technology have now emerged from their initial stages in which the basic physical mechanisms and possible applications were elucidated (only optical methods form an exception to this). This does not, however, mean that the development of this subject is complete. On the contrary, now is the time for a detailed and systematic development of all its aspects. In particular, attainment of the present level of understanding of the physics of DNP in solid dielectrics offers us new possibilities for its application in combination with ESR, NMR, and DENR in the analysis of the finer properties of spin dynamics and magnetic relaxation (see, for example, sub-sec. E, Sec. 2). Experiments on DNP of radioactive nuclei also appear to be very promising since they can be carried out in parallel with measurements of the Mössbauer effect and the anisotropy of gamma emission. The extension of the ideas and methods used in DNP and thermal mixing to double NMR in a rotating coordinate frame is an independent field with extensive applied possibilities (see, for example, the paper by Pines *et al.*[161]).

Finally, much work remains to be done on highly polarized nuclear targets which will become much more accessible when the working temperature and magnetic field are reduced, and the successes so far achieved with protons are extended to other nuclei.

I am greatly indebted to my colleagues and, in particular, M. I. Rodak, G. A. Vasneva and V. V. Demidov for stimulating support and valuable suggestions.

[1]A. W. Overhauser, Phys. Rev. **92**, 422 (1953).
[2]Proc. Second Intern. Conf. on Polarized Targets, Berkeley, 1971 (ed. by G. Shapiro) LBL 500, UC-34 Physics - Springfield, Va.: National Tech. Inform. Service, 1972.
[3]M. Goldman, M. Chapellier, Vu Hoang Chau, and A. Abragam, Phys. Rev. B **10**, 226 (1974).
[4]M. Goldman, Spin Temperature and NMR in Solids, Oxford University Press, 1970 (Russ. Transl., Mir, M., 1972).
[5]A. Abragam, The Principles of Nuclear Magnetism, Oxford University Press, 1961 (Russ. Transl., IL, M., 1963).
[6]K. Jeffries, Dynamic Nuclear Orientation, Interscience, N. Y., 1963 (Russ. transl., Mir, M., 1965).
[7]G. R. Khutsishvili, Usp. Fiz. Nauk **71**, 9 (1960) [Sov. Phys. Usp. **3**, 285 (1961)].
[8]B. N. Provorotov, Zh. Eksp. Teor. Fiz.; a) **41**, 1582 (1961) [Sov. Phys. JETP **14**, 1126 (1962)]; b) **42**, 882 (1962) [Sov. Phys. JETP **15**, 611 (1962)].
[9]J. Jeener, in: Advances in Magnetic Resonance, Vol. 3 (ed. by J. Waugh), Academic Press, New York, 1968.
[10]A. Abragam and M. Borghini, in: Progress in Low Temperature Physics, Vol. 4 (ed. by C. Gorter), North-Holland, Amsterdam, 1964, p. 384.
[11]L. L. Buishvili and M. D. Zviadadze, Physica **59**, 697 (1972).
[12]A. Abragam and W. G. Proctor, C. R. Acad. Sci. **246**, 2253 (1958).
[13]A. V. Kessenikh and A. A. Manenkov, Fiz. Tverd. Tela (Leningrad) **5**, 1143 (1963) [Sov. Phys. Solid State **5**, 835 (1963)].
[14]M. A. Kozhushner, Zh. Eksp. Teor. Fiz. **56**, 246 (1969) [Sov. Phys. JETP **29**, 136 (1969)].
[15]L. L. Buishvili, Zh. Eksp. Teor. Fiz. **49**, 1868 (1965) [Sov. Phys. JETP **22**, 1277 (1966)].
[16]M. Borghini, Phys. Lett. A **26**, 242 (1968).
[17]E. Erb, J. L. Motchane, and J. Uebersfeld, C. R. Acad. Sci. **246**, 2120, 3050 (1958).
[18]J. L. Motchane, Ann. Phys. (Paris) **7**, 139 (1962).
[19]N. Bloembergen, Physica (Utrecht) **16**, 386 (1949).
[20]G. R. Khutsishvili, a) Usp. Fiz. Nauk **87**, 211 (1965) [Sov. Phys. Usp. **8**, 743 (1966)] b) in: Polarization of Nuclei by the Solid Effect: Phys. Gesellschaft der DDR Berlin, 1972, p. 33.
[21]G. R. Khutsishvili, Usp. Fiz. Nauk **96**, 441 (1968) [Sov. Phys. Usp. **11**, 802 (1969)].
[22]M. Borghini, Phys. Rev. Lett. **16**, 318 (1966).
[23]P. G. De Gennes, J. Phys. Chem. Solids **3**, 345 (1958).
[24]G. R. Khutsishvili, Tr. Inst. Fiz. Akad. Nauk Georgian SSR **2**, 115 (1954); **4**, 3 (1956); Zh. Eksp. Teor. Fiz. **31**, 424 (1956) [Sov. Phys. JETP **4**, 382 (1957)].
[25]W. E. Blumberg, Phys. Rev. **119**, 79 (1960).
[26]G. R. Khutsishvili, Zh. Eksp. Teor. Fiz. **43**, 2179 (1962) [Sov. Phys. JETP **16**, 1540 (1963)].
[27]L. L. Buishvili and D. N. Zubarev, Fiz. Tverd. Tela (Leningrad) **7**, 722 (1965) [Sov. Phys. Solid State **7**, 580 (1965)].
[28]I. J. Lowe and D. Tse, Phys. Rev. **166**, 279 (1968).
[29]E. P. Horvits, Ditto, B **3**, 2868 (1971).
[30]R. Kh. Sabirov, Izv. Vyssh. Uchebn. Zaved. Fiz. No. 11,

76 (1975).
[31]L. L. Buishvili, M. D. Zviadadze, and B. D. Mikaberidze, Zh. Eksp. Teor. Fiz. 69, 2118 (1975) [Sov. Phys. JETP 42, 1077 (1976)].
[32]A. V. Kessenikh, V. I. Lushchikov, A. A. Manenkov, and Yu. V. Taran, Fiz. Tverd. Tela (Leningrad) 5, 443 (1963) [Sov. Phys. Solid State 5, 321 (1963)]; A. V. Kessenikh, A. A. Manenkov, and G. I. Pyatnitskiĭ, Fiz. Tverd. Tela (Leningrad) 6, 827 (1964) [Sov. Phys. Solid State 6, 641 (1964)].
[33]C. F. Hwang and D. A. Hill, Phys. Rev. Lett. 19, 1011 (1967).
[34]L. Morimoto, J. Phys. Soc. Jpn. 35, 1297, 1305 (1973).
[35]N. Bloembergen, S. Shapiro, P. S. Perschan, and J. O. Artman, Phys. Rev. 114, 445 (1959).
[36]O. Leifson and E. Vogel, *ibid.* B 2, 4266 (1970).
[37]D. W. Wollan, *ibid.* 13, 3671 (1976).
[38]M. A. Kozhushner and B. N. Provotorov, In Radiospektroskopiya tverdogo tela: Trudy Vsesoyuznogo soveshchaniya po issledovaniyu svoĭstv tverdogo tela metodami magnitnogo rezonansa, Krasnoyarsk, 1964 (in: Radio-frequency Spectroscopy of Solids. Proc. All-Union Conf. on the Properties of Solids Studied by Magnetic Resonance Methods, Krasnoyarsk, 1964), Atomizdat, M. 1967, p. 5.
[39]M. Borghini, Phys. Rev. Lett. 20, 419 (1968).
[40]M. Borghini, See Ref. 2, p. 1.
[41]V. A. Atsarkin and M. I. Rodak, Usp. Fiz. Nauk 107, 3 (1972) [Sov. Phys. Usp. 15, 251 (1972)].
[42]L. L. Buishvili and M. D. Zviadadze, Phys. Lett. A 24, 661 (1967).
[43]M. G. Melikiya, Fiz. Tverd. Tela (Leningrad) 10, 858 (1968) [Sov. Phys. Solid State 10, 673 (1968)].
[44]A. D. Milov, K. M. Salikhov, and Yu. D. Tsvetkov, Fiz. Tverd. Tela (Leningrad) 14, 2259 (1972) [Sov. Phys. Solid State 14, 1956 (1973)]; K. M. Salikov, A. G. Semenov, and Yu. D. Tsvetkov, Elektronnoe spinovoe ekho i ego primenenie (Electron Spin Echo and Its Applications), Nauka, Novosibirsk, 1976, p. 122.
[45]T. J. S. Swanenburg, G. M. Van den Heuvel, and N. J. Poulis, Physica 33, 707 (1967).
[46]A. E. Mefed, Fiz. Tverd. Tela (Leningrad) 16, 2012 (1974) [Sov. Phys. Solid State 16, 1308 (1975)].
[47]A. M. Portis, Phys. Rev. 91, 1071 (1953).
[48]A. Kiel, *ibid.* 125, 1451 (1962).
[49]L. L. Buishvili, M. D. Zviadadze, and G. R. Khutsishvili, Zh. Eksp. Teor. Fiz. 56, 290 (1969) [Sov. Phys. JETP 29, 159 (1969)].
[50]D. S. Wollan and J. W. Poulton, Phys. Lett. A 33, 33 (1970).
[51]P. Zegers, Z. Naturforsch. Teil A 24, 1737 (1969).
[52]M. Chapellier, Vu Hoang Chau, and M. Goldman, Phys. Lett. A 26, 262 (1968).
[53]P. Zegers and R. Van Steenwinkel, Physica (Utrecht) 33, 332 (1967).
[54]L. L. Buishvili, M. D. Zviadadze, and G. R. Khutsishvili, Zh. Eksp. Teor. Fiz. 54, 876 (1968) [Sov. Phys. JETP 27, 469 (1968)]; L. L. Buishvili, M. D. Zviadadze, and N. P. Fokina, Phys. Status Solidi B 54, 401 (1972).
[55]W. T. Wenckebach, T. J. B. Swanenburg, and N. J. Poulis, Physica (Utrecht) 46, 303 (1970).
[56]M. I. Rodak, Zh. Eksp. Teor. Fiz. 61, 832 (1971) [Sov. Phys. JETP 34, 443 (1972)].
[57]S. Clough and C. A. Scott, J. Phys. C 1, 919 (1968).
[58]N. S. Bendiashvili, L. L. Buishvili, and M. D. Zviadadze, Zh. Eksp. Teor. Fiz. 58, 597 (1970) [Sov. Phys. JETP 31, 321 (1970)].
[59]M. Goldman, S. F. Cox, and V. Bouffard, J. Phys. C 7, 2940 (1974).
[60]M. I. Rodak, Fiz. Tverd. Tela (Leningrad) 6, 521 (1964) [Sov. Phys. Solid State 6, 409 (1964)].
[61]J. Lambe, N. Laurance, E. C. McIrvine, and R. W. Terhune, Phys. Rev. 122, 1161 (1961).
[62]O. S. Leifson and C. D. Jeffries, *ibid.* 1781.
[63]W. T. Wenckebach, L. A. H. Schreurs, H. Hoogstraate, T. J. B. Swanenburg, and N. J. Poulis, Physica (Utrecht) 52, 455 (1971).
[64]L. L. Buishvili, M. D. Zviadadze, and N. P. Fokina, Zh. Eksp. Teor. Fiz. 65, 2272 (1973) [Sov. Phys. JETP 38, 1135 (1974)].
[65]T. J. Schmugge and C. D. Jeffries, Phys. Rev. A 138, 1785 (1965).
[66]W. De Boer, J. Low Temp. Phys. 22, 185 (1976).
[67]L. L. Buishvili, N. P. Giordadze, and A. A. Davituliani, Zh. Eksp. Teor. Fiz. 67, 161 (1974) [Sov. Phys. JETP 40, 82 (1975)].
[68]M. Odehnal and V. Bouffard, J. Phys. (Paris) 32, 699 (1971).
[69]B. W. Faughan and M. W. P. Strandberg, J. Phys. Chem. Solids 19, 155 (1961).
[70]M. Borghini, Phys. Lett. 20, 228 (1966).
[71]L. L. Buishvili and N. P. Giorgadze, Izv. Vyssh. Uchebn. Zaved. Radiofiz. 14, 1493 (1971).
[72]J. C. Gill and N. P. Viall, J. Phys. C 2, 1512 (1969).
[73]S. A. Al'tshuler, R. M. Valishev, B. N. Kochelaev, and A. Kh. Khasanov, Zh. Eksp. Teor. Fiz. 62, 639 (1972) [Sov. Phys. JETP 35, 337 (1972)].
[74]Y. Roinel and V. Bouffard, J. Magn. Reson. 18, 304 (1975).
[75]A. Abragam, V. Bouffard, and Y. Roinel, *ibid.* 22, 53 (1976).
[76]D. S. Wollan, Phys. Rev. B 13, 3686 (1976).
[77]C. F. Hwang and D. A. Hill, Phys. Rev. Lett. 18, 110 (1967).
[78]L. L. Buishvili and M. D. Zviadadze, Pis'ma Zh. Eksp. Teor. Fiz. 6, 665 (1967) [JETP Lett. 6, 153 (1967)].
[79]D. S. Wollan and H. J. Stapleton, Phys. Rev. 163, 207 (1967).
[80]V. A. Atsarkin, A. E. Mefed, and M. I. Rodak, Pis'ma Zh. Eksp. Teor. Fiz. 6, 942 (1967) [JETP Lett. 6, 359 (1967)].
[81]V. A. Atsarkin, A. E. Mefeod, and M. I. Rodak, Phys. Lett. A 27, 57 (1968).
[82]V. A. Atsarkin, M. E. Mefed, and M. I. Rodak, Zh. Eksp. Teor. Fiz. 55, 1671 (1968) [Sov. Phys. JETP 28, 877 (1969)].
[83]V. A. Atsarkin and M. I. Rodak, Fiz. Tverd. Tela (Leningrad) 11, 613 (1969) [Sov. Phys. Solid State 11, 493 (1969)].
[84]V. A. Atsarkin, Fiz. Tverd. Tela (Leningrad) 12, 1775 (1970) [Sov. Phys. Solid State 12, 1405 (1970)].
[85]V. A. Atsarkin, Zh. Eksp. Teor. Fiz. 64, 1087 (1973) [Sov. Phys. JETP 37, 552 (1973)].
[86]V. A. Atsarkin and O. A. Ryabushkin, Pis'ma Zh. Eksp. Teor. Fiz. 17, 103 (1973) [JETP Lett. 17, 71 (1973)].
[87]V. A. Atsarkin, O. A. Ryabushkin, and V. A. Skidanov, Zh. Eksp. Teor. Fiz. 72, 1118 (1977) [Sov. Phys. JETP 45, 584 (1977)].
[88]H. H. Niebuhr, E. E. Hundt, and E. Brun, Helv. Phys. Acta 43, 777 (1970).
[89]V. A. Atsarkin, Zh. Eksp. Teor. Fiz. 59, 769 (1970) [Sov. Phys. JETP 32, 421 (1971)].
[90]T. J. B. Swanenburg, G. M. Van den Heuvel, and N. J. Poulis, Physica (Utrecht) 35, 369 (1967).
[91]W. T. Wenckebach, T. J. B. Swanenburg, and N. J. Poulis, Phys. Rept. 14, 183 (1974).
[92]W. T. Wenckebach, G. M. Van den Heuvel, H. Hogstraate, T. J. B. Swanenburg, and N. J. Poulis, Phys. Rev. Lett. 22, 581 (1969).
[93]W. T. Wenckebuch, T. J. B. Swanenburg, and N. J. Poulis, Physica (Utrecht) 50, 289 (1970).
[94]G. Hoogstraate, J. Van Houten, L. A. H. Schreurs, W. T. Wenkebuch, and N. J. Poulis, *ibid.* 65, 347 (1973).
[95]W. T. Wenckebach, T. J. W. Swanenburg, H. Hoogestraate, and N. J. Poulis, Phys. Lett. A 26, 203 (1968).
[96]M. Borghini and J. Scheffler, Phys. Rev. Lett. 26, 1362 (1971).
[97]W. De Boer, M. Borghini, K. Morimoto, and T. O. Niini-

koski, J. Low Temp. Phys. 15, 249 (1974).
[98]S. F. J. Cox, V. Bouffard, and M. Goldman, J. Phys. C 6, L100 (1973).
[99]V. A. Atsarkin, G. A. Vasneva, and E. A. Novikov, Zh. Eksp. Teor. Fiz. 68, 1491 (1975) [Sov. Phys. JETP 41, 746 (1975)].
[100]M. Borghini, W. De Boer, and K. Morimoto, Phys. Lett. A 48, 244 (1975).
[101]J. Avalos, B. Marticorena, and E. Volino, *ibid.* 51, 428 (1975).
[102]J. C. Henaux and J. Conard, in: Magnetic Resonance and Related Phenomena. Proc. Seventeenth Congress AMPERE, Turku (ed. by V. Hovi), North-Holland, Amsterdam, 1973.
[103]M. Odehnal, V. I. Loutchikov, and J. Ezratty, J. Phys. (Paris) 29, 941 (1968).
[104]B. S. Neganov, L. B. Parfenov, V. I. Lushchikov, and Yu. V. Taran, Zh. Eksp. Teor. Fiz. 45, 394 (1963) [Sov. Phys. JETP 18, 273 (1964)].
[105]D. A. Hill, B. A. Hasher, and C. F. Hwang, Phys. Lett. 23, 63 (1966).
[106]J. Burget, V. Petricek, J. Sacha, and R. Tichy, Czech. J. Phys. 17, 1041 (1967).
[107]E. I. Bunyatova, Yu. F. Kiselev, B. S. Neganov, L. B. Parfenov, É. G. Rozantsev, V. B. Stryukov, and G. Feller, Preprint No. R6-7408, Joint Institute for Nuclear Research, Dubna, 1973.
[108]K. Grude and W. Muller-Warmuth, Z. Naturforsch. Teil A 24, 1532 (1969).
[109]H. Glättli, M. Odehnal, J. Ezratty, A. Malinovski, and A. Abragam, Phys. Lett. A 29, 250 (1969).
[110]S. Mango, O. Runolfsson, and M. Borghini, Nucl. Instrum. Methods 72, 45 (1969).
[111]N. S. Garif'yanov, B. M. Kozyrev, and V. N. Fedotov, Dokl. Akad. Nauk SSSR 178, 808 (1968) [Sov. Phys. Dokl. 13, 107 (1968)].
[112]V. A. Atsarkin, P. E. Budkovskiĭ, G. A. Vasneva, V. V. Demidov, E. A. Novikov, O. A. Ryabushkin, and Yu. V. Funtikov, Fiz. Tverd. Tela (Leningrad) 15, 843 (1973) [Sov. Phys. Solid State 15, 580 (1973)].
[113]M. Borghini, O. Chamberlain, R. Z. Fuzesy, W. Gorn, C. C. Morehouse, T. Powell, P. Robrish, S. Rock, S. Shannon, G. Shapiro, and H. Weisberg, Nucl. Instrum. Methods 84, 68 (1970).
[114]A. Masaike, H. Glättli, J. Ezratty, and A. Malinovskii, Phys. Lett. A 30, 63 (1969).
[115]W. De Boer, Nucl. Instrum. Methods 107, 99 (1973).
[116]W. De Boer and T. O. Niinikosi, *ibid.* 114, 495 (1974).
[117]P. Weymuth, see Ref. 2, p. 301.
[118]M. Borghini, T. O. Niinikosi, F. Udo, and P. Weimuth, Nucl. Instrum. Methods 105, 215 (1972).
[119]D. A. Hill, J. B. Ketterson, R. C. Miller, A. Moretti, R. C. Niemann, L. R. Windmiller, A. Yokosawa, and C. F. Hwang, Phys. Rev. Lett. 23, 460 (1969).
[120]D. J. Nicholas, P. H. T. Banks, and D. A. Cragg, Nucl. Instrum. Methods 88, 69 (1970).
[121]S. Mango, see Ref. 2, p. 984.
[122]G. Harmann, D. Hubert, S. Mango, C. C. Morehouse, and K. Plog, Nucl. Instrum. Methods 106, 9 (1973).
[123]D. J. Nicholas, W. G. Williams, P. H. T. Banks, and D. A. Cragg, *ibid.* 87, 30 (1970).
[124]K. Scheffler, *ibid.* 82, 205 (1970).
[125]P. J. Bendt, Phys. Rev. B 2, 4375 (1970).
[126]Y. Roinel, V. Bouffard, and H. Glättli, C. R. Acad. Sci. Ser B 281, 113 (1975).
[127]H. M. Bozler, J. A. Brown, and E. H. Craf, Bull. Am. Phys. Soc. 18, 545 (1973).
[128]M. Borghini and K. Scheffler, Nucl. Instrum. Methods 95, 93 (1974).
[129]W. De Boer and K. Scheffler, *ibid.* W. De Boer, in: Proc. First Special Congress AMPERE, Cracow (ed. by J. Hennel), 1973, p. 228.
[130]T. O. Niinikoski and F. Udo, Nucl. Instrum. Methods 134, 219 (1976).
[131]M. Borghini, A. Masaike, K. Scheffler, and F. Udo, *ibid.* 97, 577 (1971).
[132]A. Honig and H. Mano, Phys. Rev. B 14, 1858 (1976).
[133]M. Chapellier, M. Goldman, Vu Hoang Chau, and A. Abragam, C. R. Acad. Sci. Ser. B 268, 1530 (1969); J. Appl. Phys. 41, 849.
[134]J. F. Jackuinot, W. T. Wenckebach, M. Chapellier, M. Goldman, and A. Abragam, C. R. Acad. Sci. Ser. B 278, 93 (1974).
[135]S. F. J. Cox, V. Bouffard, and M. Goldman, J. Phys. Ser. C 8, 3664 (1975).
[136]V. G. Pokazan'ev, G. V. Skrotskiĭ, and L. I. Yakub, Usp. Fiz. Nauk 116, 485 (1975) [Sov. Phys. Usp. 7, 533 (1976)].
[137]A. Abragam, Physica (Utrecht) 76–88, 1066 (1977).
[138]A. Abragam, G. L. Bacchella, H. Glättli, P. Meriel, J. Piesvaux, and M. Pinot, C. R. Acad. Sci. Ser. B 274, 423 (1972).
[139]E. E. Hundt, H. H. Niebuhr, B. Derigetti, and E. Brun, in: Magnetic Resonance and Related Phenomena. Proc. Sixteenth Congress AMPERE, Bucharest (ed. by I. Ursu), Bucharest, 1971, p. 953.
[140]C. Gabathuler and E. Brun, Helv. Phys. Acta 47, 432 (1974).
[141]S. Lee, Phys. Lett. A 266, 572 (1968).
[142]K. Muto and H. Hirakawa, J. Phys. Soc. Jpn. 42, 1467 (1977).
[143]S. Lee, R. K. Jeck, and V. P. Jacobsmeyer, Phys. Rev. Lett. 21, 515 (1968).
[144]H. H. Niebuhr, E. E. Hundt, and E. Brun, *ibid.* 1735.
[145]C. M. Brodbeck, H. H. Niebuhr, and S. Lee, Phys. Rev. B 5, 19 (1971).
[146]C. M. Brodbeck, S. Lee, and H. H. Niebuhr, *ibid.* 10, 844 (1974).
[147]S. Lee, C. M. Brodbeck, and C. C. Yang, *ibid.* 15, 2469 (1977).
[148]V. A. Golenishchev-Kutuzov, R. V. Saburova, and N. A. Shamukov, Usp. Fiz. Nauk 119, 201 (1976) [Sov. Phys. Usp. 19, 449 (1976)].
[149]G. V. H. Wilson, H. Hore, D. H. Chaplin, H. R. Foster, and E. P. George, in: Laser Interaction and Related Plasma Phenomena. Proc. Fourth Intern. Conf., Troy, N. Y., 1976.
[150]J. Leblond, J. L. Motchane, P. Panon, and J. Uebersfeld, C. R. Acad. Sci. Ser. B 265, 432 (1967).
[151]J. Leblond, J. Uebersfeld, and J. Korringa, Phys. Rev. A 4, 1532 (1971).
[152]P. Panon, J. L. Motchane, and J. Korringa, *ibid.* 175, 641 (1968).
[153]L. Deutschebein, H. Gotz, H. Schulze, and K. Werner, Phys. Status Solidi B 56, 101 (1973).
[154]H. Schuch, D. Stehlik, and K. H. Hausser, Z. Naturforsch. Teil A 26, 1944 (1971).
[155]C. D. Jeffries, Phys. Rev. Lett. 19, 1221 (1967).
[156]W. B. Grant, L. F. Mollenauer, and C. D. Jeffries, Phys. Rev. B 4, 1428 (1971).
[157]J. P. Colpa, K. H. Hausser, and D. Stehlik, Z. Naturforsch. Teil A 26, 1972 (1971).
[158]P. Lau, D. Stehlik, and K. H. Hausser, J. Magn. Reson. 8, 85 (1976).
[159]K. H. Hausser and H. C. Wolf, Adv. Magn. Reson. 8, 85 (1976).
[160]V. A. Atsarkin and S. K. Morshnev, Zh. Eksp. Teor. Fiz. 71, 1520 (1976) [Sov. Phys. JETP 44, 795 (1976)].
[161]A. Pines, M. G. Gibby, and J. S. Waugh, J. Chem. Phys. 59, 569 (1973).

Translated by S. Chomet